

**ISOTOPIC FRACTIONATION OF BARIUM IN SHALE AND PRODUCED WATER  
FROM THE APPALACHIAN BASIN, USA**

by

**Zachary Garrison Tieman**

B.S. Earth Science, George Mason University, 2011

Submitted to the Graduate Faculty of the  
Kenneth P. Dietrich School of Arts and Sciences in partial fulfillment  
of the requirements for the degree of  
Master of Science

University of Pittsburgh

2017

UNIVERSITY OF PITTSBURGH  
KENNETH P. DIETRICH SCHOOL OF ARTS AND SCIENCES

This thesis was presented

by

Zachary Garrison Tieman

It was defended on

November 30, 2017

and approved by

Rosemary Capo, Associate Professor, Department of Geology and Environmental Science

Charles E. Jones, Senior Lecturer, Department of Geology and Environmental Science

Josef Werne, Professor, Department of Geology and Environmental Science

Thesis Advisor: Brian Stewart, Associate Professor, Department of Geology and Environmental  
Science

ISOTOPIC FRACTIONATION OF BARIUM IN SHALE AND PRODUCED WATER FROM  
THE APPALACHIAN BASIN, USA

Zachary Garrison Tieman, MS

University of Pittsburgh, 2017

Waters co-produced with oil and gas are often rich in barium (Ba), which can cause scale formation and fouling of wells, especially in unconventional Marcellus Shale gas wells. To address the source of barium in these produced waters, Ba isotope ratios were determined on returned water samples from a Marcellus Shale gas well in West Virginia and other oil- and gas-producing units in Pennsylvania, as well as on exchangeable and carbonate Ba from core samples. This study presents the first known measurements of barium isotopes in produced waters from conventional and unconventional wells and from shale core material. Previous studies have shown that the lighter isotopes of Ba are preferentially fractionated into solid aqueous Ba-rich minerals (*e.g.*, barite, BaSO<sub>4</sub>, and witherite, BaCO<sub>3</sub>), and that Ba isotopes can be fractionated by biological and cation exchange processes.. A methodology for measuring stable barium isotope ratios is presented, including separation of Ba from the matrix and using a double spike to correct for mass fractionation. Barium isotope ratios are reported as  $\delta^{138}\text{Ba}$ , the permil (‰) deviation of the  $^{138}\text{Ba}/^{134}\text{Ba}$  ratio from NIST standard SRM 3104a. A time series of produced water from the hydraulically fractured Marcellus well yielded values ranging from

$\delta^{138}\text{Ba} = 0.81\text{‰}$  to  $1.01\text{‰}$  (typical uncertainty  $\pm 0.06\text{‰}$  or better). In contrast, the barium found in the exchangeable sites of Marcellus rock, the largest source of labile Ba, varied from  $0.45\text{‰}$  to  $0.60\text{‰}$ , significantly lower than the produced water, suggesting that Ba in produced water is not sourced from shale exchange sites. The carbonate fractions from the same rocks had similar values but lower Ba concentrations by a factor of  $10^2$ . Produced water from Marcellus Shale wells in different geographic locations (Greene, Westmoreland and Tioga Counties, PA) yield similar  $\delta^{138}\text{Ba}$  values, although the Westmoreland Co. sample had a higher value ( $1.50\text{‰}$ ). In contrast, waters derived from units both below and above the Marcellus shale yielded significantly lower  $\delta^{138}\text{Ba}$  values, ranging from  $-0.81\text{‰}$  to  $0.09\text{‰}$ . This system shows promise as a means of differentiating fluids migrating from Marcellus Shale wells from those of nearby conventional oil and gas wells.

## TABLE OF CONTENTS

<b>1.0</b>	<b>INTRODUCTION</b>	<b>1</b>
<b>1.1</b>	<b>THESIS OVERVIEW</b>	<b>1</b>
<b>1.2</b>	<b>PRODUCED WATERS IN THE APPALACHIAN BASIN</b>	<b>2</b>
<b>1.2.1</b>	<b>Conventional and unconventional oil and gas wells</b>	<b>2</b>
<b>1.2.2</b>	<b>Appalachian basin produced water chemistry</b>	<b>4</b>
<b>1.2.3</b>	<b>Barium in produced water</b>	<b>5</b>
<b>1.3</b>	<b>BARIUM AND BA ISOTOPES IN NATURAL SYSTEMS</b>	<b>6</b>
<b>1.3.1</b>	<b>Occurrence of Ba in Earth's crust and near-surface environment</b>	<b>6</b>
<b>1.3.2</b>	<b>Barium isotope systematics</b>	<b>8</b>
<b>1.3.3</b>	<b>Ba isotope fractionation from mineral precipitation and dissolution</b>	<b>9</b>
<b>1.3.4</b>	<b>Ba isotope variations in igneous rock and river water</b>	<b>11</b>
<b>1.3.5</b>	<b>Fractionation from biologically driven processes</b>	<b>11</b>
<b>1.3.6</b>	<b>Ba isotope fractionation from other processes</b>	<b>14</b>
<b>2.0</b>	<b>BARIUM ISOTOPE METHOD DEVELOPMENT</b>	<b>15</b>
<b>2.1</b>	<b>OVERVIEW OF BA ISOTOPE MEASUREMENT METHODOLOGY AND REQUIREMENTS</b>	<b>15</b>
<b>2.2</b>	<b>CATION EXCHANGE COLUMN SEPARATION OF BA</b>	<b>15</b>
<b>2.2.1</b>	<b>Sample preparation</b>	<b>15</b>

2.2.2	Columns and cation exchange resin .....	16
2.2.3	Column calibration .....	17
2.2.3.1	Produced water calibration curves .....	17
2.2.3.2	Sequential extraction calibration curves .....	18
2.3	<b>BARIUM DOUBLE SPIKE .....</b>	<b>23</b>
2.3.1	Theory .....	23
2.3.2	Choice of spike isotopes .....	23
2.3.3	Calculating sample $^{138}\text{Ba}/^{134}\text{Ba}$ from isotope ratio measurements .	26
2.4	<b>ANALYSIS BY MC-ICP-MS .....</b>	<b>30</b>
2.4.1	Run parameters .....	30
2.4.2	Isobaric interference corrections .....	31
2.4.3	Data evaluation .....	33
3.0	<b>BARIUM ISOTOPE VARIATIONS IN THE MARCELLUS SHALE AND APPALACHIAN BASIN PRODUCED WATERS .....</b>	<b>34</b>
3.1	<b>INTRODUCTION .....</b>	<b>34</b>
3.2	<b>GEOLOGY OF THE MARCELLUS SHALE .....</b>	<b>36</b>
3.3	<b>SAMPLE MATERIALS .....</b>	<b>37</b>
3.3.1	Core and produced water from the MSEEL drilling site .....	37
3.3.2	Produced water from other sites .....	41
3.4	<b>METHODS .....</b>	<b>42</b>
3.4.1	Sequential extraction .....	42
3.4.2	Chemistry and mass spectrometry .....	43
3.5	<b>RESULTS .....</b>	<b>43</b>

3.5.1	Shale leachates .....	43
3.5.2	Produced waters .....	45
3.6	DISCUSSION .....	51
3.6.1	Source of Ba in shale produced water .....	51
3.6.2	Source of Ba in shale exchangeable sites and carbonates .....	52
3.6.3	Ba isotope variations in produced water .....	53
4.0	CONCLUSIONS .....	54
	APPENDIX .....	56
	BIBLIOGRAPHY .....	60

## LIST OF TABLES

Table 1: Abundances and isobaric interferences for barium and overlapping isotopes . . . . .	25
Table 2: $\delta^{138}\text{Ba}$ of extracted samples . . . . .	44
Table 3: $\delta^{138}\text{Ba}$ of produced waters . . . . .	49

## LIST OF FIGURES

Figure 1: Diagram of conventional vs. unconventional well (MNGD and MRH, 2017) .....	3
Figure 2: Overview of $\delta^{138}\text{Ba}$ literature values (von Allmen et al., 2010; Bullen and Chadwick, 2015; Cao et al., 2015; Horner et al., 2015; Nian et al., 2015; Pretet et al., 2015) .....	10
Figure 3: Trend of barium concentration and $\delta^{138}\text{Ba}$ with ocean depth, south Atlantic Ocean, 39.99d S, 0.92d E (Horner et al., 2015) .....	13
Figure 4: Cation separation using different resin heights .....	19
Figure 5: Final produced water elution curve of Ba, major elements, and potential REE isobaric interferences (La and Ce) using 6 cm resin heights .....	20
Figure 6: Elution curves of selected elements in produced waters using different acids after the first 13.5 mL of 2.0 N HCl were added .....	21
Figure 7: First and second elutions of sequentially extracted barium. In the second run, Ba from the first column (15-38 mL) was put through a second column with new resin .....	22
Figure 8: The isotope abundances of an optimally-spiked sample .....	24
Figure 9: Error curves for the proportions of $^{135}\text{Ba}$ (spike 4) and $^{137}\text{Ba}$ (spike 6) and for the proportions of double spike and sample. Left is optimized for measurement of $^{138}\text{Ba}/^{134}\text{Ba}$ ; right is optimized for measurement of $^{138}\text{Ba}/^{136}\text{Ba}$ . Created using the double spike toolbox (Rudge et al., 2009; <a href="http://www.johnrudge.com/doublespike">http://www.johnrudge.com/doublespike</a> ) .....	25
Figure 10: Measurements of standard during MC-ICP-MS runs; (a) initial runs (b) with Apex introduction system .....	32

Figure 11: Depth and thickness map of the Marcellus Shale, with a 50 ft. isopach contour, a 1500 ft. depth contour, and sampling areas marked: M - MSEEL, G - Greene Co., W - Westmoreland Co., T - Tioga Co. (modified from Wang and Carr, 2013) ..... 35

Figure 12: Cambrian through Permian stratigraphy in Pennsylvania (modified from Rowan et al., 2015) ..... 38

Figure 13: Paleographic reconstruction of North America, Middle Devonian; approximate paleolocation of study areas marked (modified from Blakey, 2017) ..... 39

Figure 14: MSEEL well site and schematic near Morgantown, WV (MSEEL, 2017) ..... 40

Figure 15: Summary of  $\delta^{138}\text{Ba}$  results with some comparative literature values. Conventional well samples are diamonds, unconventional are squares, leachates are triangles. Data not from this study are from von Allmen et al., 2010, Bullen and Chadwick, 2015, Cao et al., 2015, Horner et al., 2015, Nan et al., 2015, and Pretet et al., 2015) ..... 46

Figure 16:  $\delta^{138}\text{Ba}$  of leachates by depth ..... 47

Figure 17: Correlation of exchangeable and carbonate  $\delta^{138}\text{Ba}$  with Ba concentration (ug of Ba per g of sample leached) ..... 48

Figure 18: Plot of (a) [Ba] and (b)  $\delta^{138}\text{Ba}$  against day of sample collection after initiation of flowback for the MSEEL 3H well; range of  $\delta^{138}\text{Ba}$  values for the cation leachates shown in the shaded area ..... 50

## **1.0 INTRODUCTION AND BACKGROUND**

### **1.1 THESIS OVERVIEW**

The pore spaces and capillaries of deep sedimentary basins—the most common sources of oil and natural gas—often contain aqueous fluids that have greater levels of total dissolved solids (TDS) than seawater (Land, 1995) and that may have been there for millions of years. When hydrocarbons are pumped from these formations, chloride-rich brines, here referred to as produced waters, are often extracted along with the oil and gas (Collins, 1975). In Pennsylvania, produced water TDS can exceed 300,000 mg/L (Poth, 1962; Dresel and Rose, 2010). High-TDS produced waters are generated both from conventional wells, in which the hydrocarbon is extracted from a permeable reservoir overlying the organic-rich source rock, and from unconventional wells, in which the organic-rich source rock (usually shale) is also the reservoir. Hydrocarbons in unconventional wells are extracted by hydraulic fracturing.

Although the composition of produced waters is dominated by sodium, barium (Ba) can make up a significant portion of the TDS. In Pennsylvania, conventional well produced waters contain up to 4,370 mg/L Ba (Dresel and Rose, 2010), while unconventional well produced water in some areas contain up to 13,800 mg/L (Barbot et al., 2013). High levels of Ba often result in precipitation of barite ( $\text{BaSO}_4$ ), a particularly insoluble scale that can reduce permeability or completely block oil and gas wells (Paukert Vankeuren et al., 2017). Therefore,

it is of major interest to understand the origin of Ba in produced waters, in particular those from unconventional reservoirs, to minimize the return of barium from the deep subsurface (Chapman et al., 2012; Stewart et al., 2015; Phan et al., 2015; Renock et al., 2016).

In this study I apply stable isotopes of Ba to address the origin of Ba in produced water from Appalachian Basin oil and gas wells. While Ba isotope variations have been measured in meteorites since the 1960s (e.g., Umemoto, 1962; Eugster et al., 1969), workers have only recently begun addressing Ba isotope fractionation resulting from Earth surface processes, primarily in the oceans (e.g., von Allmen et al., 2010; Horner et al., 2015; Bates et al., 2017). This study represents the first known investigation of Ba isotope variations in produced waters and their associated reservoir rocks.

## **1.2 PRODUCED WATERS IN THE APPALACHIAN BASIN**

### **1.2.1 Conventional and unconventional oil and gas wells**

Conventional oil and gas wells are those in which a permeable reservoir is tapped, and the overlying pressure of rock does the work in bringing hydrocarbons to the surface. The reservoir rock is porous, often sandstone, overlying an organic-rich source rock (*e.g.*, a black shale) which released its hydrocarbons upwards into the reservoir. Folds or faults of an impermeable rock, generally shale, create an impermeable barrier that allows the oil to accumulate into an economic deposit (MNGD and MRH, 2017; Figure 1). Pumping or other methods may be used to assist oil recovery (Terry, 2001).

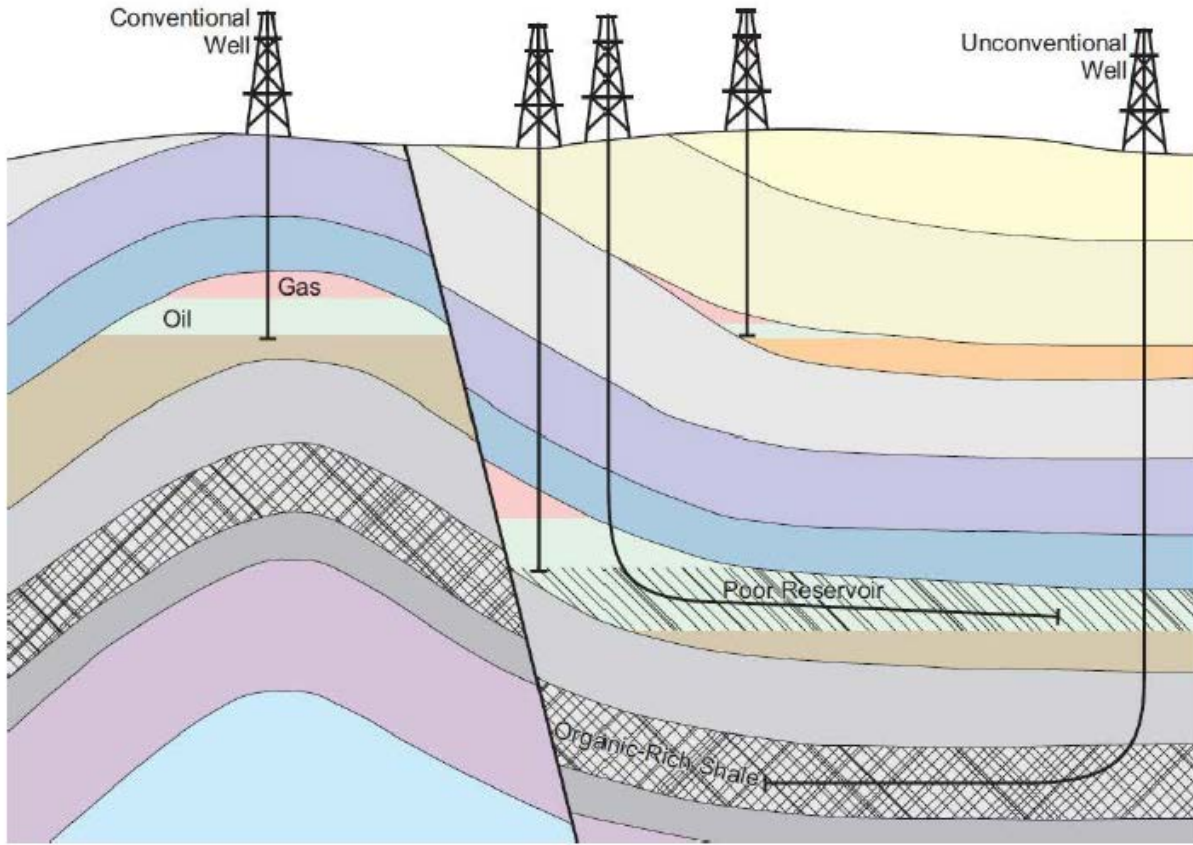


Figure 1: Diagram of conventional vs. unconventional well (from MNGD and MRH, 2017)

Unconventional wells extract hydrocarbons directly from the source rock (MNGD and MRH, 2017). In Pennsylvania, this is most commonly done through hydraulic fracturing. A well bore drills to the targeted formation and then goes through it laterally for thousands of feet (Rowan et al., 2015). Fracking fluid, primarily water and sand, but also bearing a combination of chemicals to inhibit scaling and aid in other functions (Soeder et al., 2014), is pumped into the formation at high pressures to fracture the surrounding formation and release the bound hydrocarbons. In the Appalachian Basin the Middle Devonian Marcellus Shale has been the primary target of unconventional natural gas extraction (Zagorski et al., 2012).

For approximately the first two weeks after hydraulic stimulation, the fluid returning to the surface, called flowback, rapidly decreases in volume over time and increases in TDS. The oxygen isotope composition also shifts from one similar to what was injected into the well to a distinct value that typically plateaus about a year after initial flowback; this is thought to be the  $\delta^{18}\text{O}$  of the formation water (Rowan et al., 2015). After 2-3 weeks, the returning brine approaches an asymptotic plateau of TDS and chemical concentration (Haluszczak et al., 2012; Capo et al., 2014). Flowback and formation water both fall under the umbrella term produced water (Engle and Rowan, 2014).

### **1.2.2 Appalachian basin produced water chemistry**

Within the Appalachian Basin, formation waters are primarily Na-Ca-Cl brines (Rowan et al., 2015) thought to be paleoseawater, evaporated beyond halite saturation with a varying amount of meteoric water mixed in, especially along the northwestern edge where Pleistocene glacier melt has infiltrated the basin (Dresel and Rose, 2010; Engle and Rowan, 2014). Appalachian Basin formation waters may also have been affected by water-rock interaction and microbial activity (Haluszczak et al., 2012; McIntosh et al., 2004). The produced waters throughout the

Appalachian Basin have a TDS of 100,000 to 300,000 mg/L (Rowan et al., 2015) and generally show linear correlations of sodium, calcium, magnesium, and bromine (Dresel and Rose, 2010). Brines produced from unconventional wells share a broadly similar major element chemistry and similar Na:Cl ratio to those from conventional wells within the Appalachian Basin, although trace element signatures within Marcellus Shale produced waters are distinct (Barbot et al., 2013; Rowan et al., 2015). Unconventional Marcellus wells return relatively high TDS and barium compared to other Appalachian basin wells, along with higher strontium, slightly less calcium, and much less magnesium (Barbot et al., 2013).

### **1.2.3 Barium in produced water**

Divalent cations within the brine—particularly calcium, strontium, and barium—react with injected water to form carbonate and sulfate mineral scaling. This is a known problem, and descalant is added to fracking solutions commonly to prevent precipitation and to break up such mineral buildup (Soeder et al., 2014). This works well with calcium carbonates and to a lesser degree carbonates containing iron and magnesium, but barite ( $\text{BaSO}_4$ ) is particularly insoluble and difficult to dissolve once formed (Shen et al., 2009).

The source of the great concentration of barium within the Marcellus Shale is unclear. Stewart et al. (2015) noted that almost all sequentially extracted Ba from core samples was from exchangeable sites and could be mobilized by water injected during hydraulic fracturing. However, very large rock:water ratios would be required to account for all of the barium seen in Marcellus produced waters. They suggested that it is possible the high TDS fluids are formation waters from sandy lenses, fractures within the Marcellus Shale, or from adjacent, more permeable units. Potentially high levels of Ba could already exist in formation water due to the highly reducing, sulfate-poor nature of the formation (Lash and Blood, 2014). Renock et al.

(2016) suggest that both Ba from barite within the shale, mobilized by high-TDS fluids, and that exchangeable barium interacts with injected fluids to generate the high levels seen in Marcellus Shale produced water.

For this study, the isotopes of barium found in produced water and selected leachates from core samples were measured in hopes that the isotopic composition could yield information about the source of barium within the shale and to provide new data in this relatively untested isotopic system. Any relationships found in formation water between the composition in seawater, early flowback, and produced waters from other formations could give valuable information in the sourcing of the barium found in Marcellus Shale produced waters.

### **1.3 BARIUM AND BA ISOTOPES IN NATURAL SYSTEMS**

#### **1.3.1 Occurrence of Ba in Earth's crust and near-surface environment**

Barium is a divalent alkaline earth metal, most often seen in minerals replacing potassium in K-feldspar and micas due to their similar ionic radii ( $\text{Ba}^{2+} = 1.35\text{\AA}$ ;  $\text{K}^+ = 1.38\text{\AA}$ ). It substitutes to a lesser extent for  $\text{Ca}^{2+}$  in plagioclase, pyroxene, amphibole, apatite, and calcite. Its most common ore is barite ( $\text{BaSO}_4$ ), which occurs in marine environments as described below, and in the secondary carbonate witherite (Salminen, 2005).

In igneous rocks, barium concentration tends to increase with silica content. Ultramafic rocks have around 0.4 ppm, basalts have 330 ppm, and granites have 200-840 ppm, while syenites often contain >1000 ppm (Salminen, 2005). The concentration in sedimentary rocks depends on the existence of K-feldspar and of clays and hydrous oxides to which it may adsorb. Carbonates and sandstones have only about 10 ppm, while shale has the highest concentrations of barium in sedimentary rocks with an average of about 580 ppm (Salminen, 2005).

While the ocean is mostly undersaturated in barite, it does occur in micrometer-sized crystals throughout the water column in areas of primary productivity and at depth. This is due to oxidation of organic carbon that occurs during decay of suspended phytoplankton, which is thought to be the primary control on barium concentration in these areas (Gonneea and Paytan, 2006; Griffith and Paytan, 2012; Lash and Blood, 2014; Horner, et al., 2015). Dissolved barium follows a nutrient-like gradient in the ocean. It is not known to have much use in phytoplankton physiological processes (Horner, et al., 2015) beyond as an impurity in processes that preferentially use calcium (Bullen and Chadwick, 2015). Barite crystals have been seen in benthic protozoa, but they are not abundant in the ocean, and the amount of barite precipitate to the total budget is probably inconsequential (Griffith and Paytan, 2012). Barium also adsorbs onto biogenic particles. Barium concentrations in pelagic environments can potentially be used as a proxy for primary productivity in the overlying water column (Cao et al., 2015; Lash and Blood, 2014).

Some marine barite is formed due to hydrothermal fluids which leach barium from basalt and mix it with sulfates in the surrounding seawater. Barite forms during the early and later stages of hydrothermal chimney growth when temperatures are cooler, and it acts as structural support, preserving the chimneys with its low solubility (Jamieson, et al., 2016). Barite may also form due to cold seeps, in which Ba-rich fluids are driven from the sediment in tectonic or hydrological processes or diagenetically as tectonics or increased load causes clastic and sediment dewatering. Oceanic environments near coastal regions may also have strong inputs of barium due to riverine dumping (Griffith and Paytan, 2012). Witherite ( $\text{BaCO}_3$ ) forms in the same areas as a secondary mineral after barite. It is, however, rare in nature and only known to occur in economic volumes in a few localities (Lü et al., 2003).

### 1.3.2 Barium isotope systematics

Barium has seven stable isotopes:  $^{130}\text{Ba}$  (0.11%),  $^{132}\text{Ba}$  (0.10%),  $^{134}\text{Ba}$  (2.42%),  $^{135}\text{Ba}$  (6.59%),  $^{136}\text{Ba}$  (7.85%),  $^{137}\text{Ba}$  (11.23%), and  $^{138}\text{Ba}$  (71.70%). The isotopic composition of barium was first measured by Nier (1938). Eugster et al. (1969) accurately determined Ba isotope composition in meteorites and terrestrial material using an isotopic double spike technique which allows correction for fractionation that occurs during sample preparation and measurement. The values of Eugster et al. (1969) were further refined by McCulloch and Wasserburg (1978). Multi-collector inductively-coupled plasma mass spectrometry (MC-ICP-MS) was first used for Ba isotope measurement by von Allmen et al. (2010) to determine precipitation-related mass fractionation. Since then, a growing number of Ba isotope studies have been carried out to investigate precipitation, dissolution, and biogenic fractionation under natural and experimental conditions (Bottcher et al., 2012; Miyazaki et al., 2014; Horner et al., 2015; Bullen and Chadwick, 2015; Nan et al., 2015; van Zuilen et al., 2016; Mavromatis et al., 2016; Cao et al., 2016; Bates et al., 2017).

Barium isotope composition is reported relative to a standard value, where the selected isotope ratio (in this study,  $^{138}\text{Ba}/^{134}\text{Ba}$ ) is normalized to the same ratio in a standard:

$$\delta^{138}\text{Ba} = \left( \frac{^{138}\text{Ba}/^{134}\text{Ba} (\text{sample})}{^{138}\text{Ba}/^{134}\text{Ba} (\text{standard})} - 1 \right) \times 1000$$

Hereafter, the  $\delta^{138/134}\text{Ba}$  will be referred to as  $\delta^{138}\text{Ba}$ . While the current most-used standard (and the one used in this study) is NIST 3104a, other standards, including IAEA standards (primarily CO-9) and a standard created by Inorganic Ventures, have also been used (Nan et al., 2015; Cao et al., 2015). Positive  $\delta^{138}\text{Ba}$  values indicate higher  $^{138}\text{Ba}/^{134}\text{Ba}$  values than the standard (the sample is “heavy”) while negative values indicate the reverse (the sample is “light”). In some

studies, the  $^{137}\text{Ba}/^{134}\text{Ba}$  ratio is reported (as  $\delta^{137}\text{Ba}$ ) rather than  $\delta^{138}\text{Ba}$ . The conversion factor can be approximated as:

$$\delta^{138}\text{Ba} \approx 1.33 \cdot \delta^{137}\text{Ba}$$

(Horner et al., 2015). The total range of  $\delta^{138}\text{Ba}$  measured in different natural materials ( $\delta^{138}\text{Ba}$  from -0.7 to 1.33‰) is shown in Figure 2 and discussed below.

### **1.3.3 Ba isotope fractionation from mineral precipitation and dissolution**

Precipitation of minerals primarily results in a preference for lighter isotopes in crystal structures with the level of fractionation affected by temperature. von Allmen et al. (2010) reported Ba isotope fractionation with variables of temperature and precipitation rate. They found a maximum isotope fractionation of -0.4‰ (when converted to  $\delta^{138}\text{Ba}$ ) between a  $\text{BaCl}_2$  solution and barite or witherite ( $\text{BaCO}_3$ ). They found only minimal temperature effects in their experimental range of 21-80°C, while precipitation rate appeared to affect isotope fractionation more strongly.

A later study (Mavromatis et al., 2016) demonstrated kinetic isotope fractionation from precipitation of witherite in an aqueous fluid. The fluid became isotopically heavier (by almost 0.3‰) as isotopically light Ba was preferentially precipitated into witherite. They found that the isotopically heavy fluid gradually equilibrated with the lighter witherite, approaching the fluid's initial isotopic composition over a period of about seven days, suggesting little to no fractionation at equilibrium. They also found that witherite dissolution resulted in no measurable Ba isotope fractionation between the mineral and fluid.

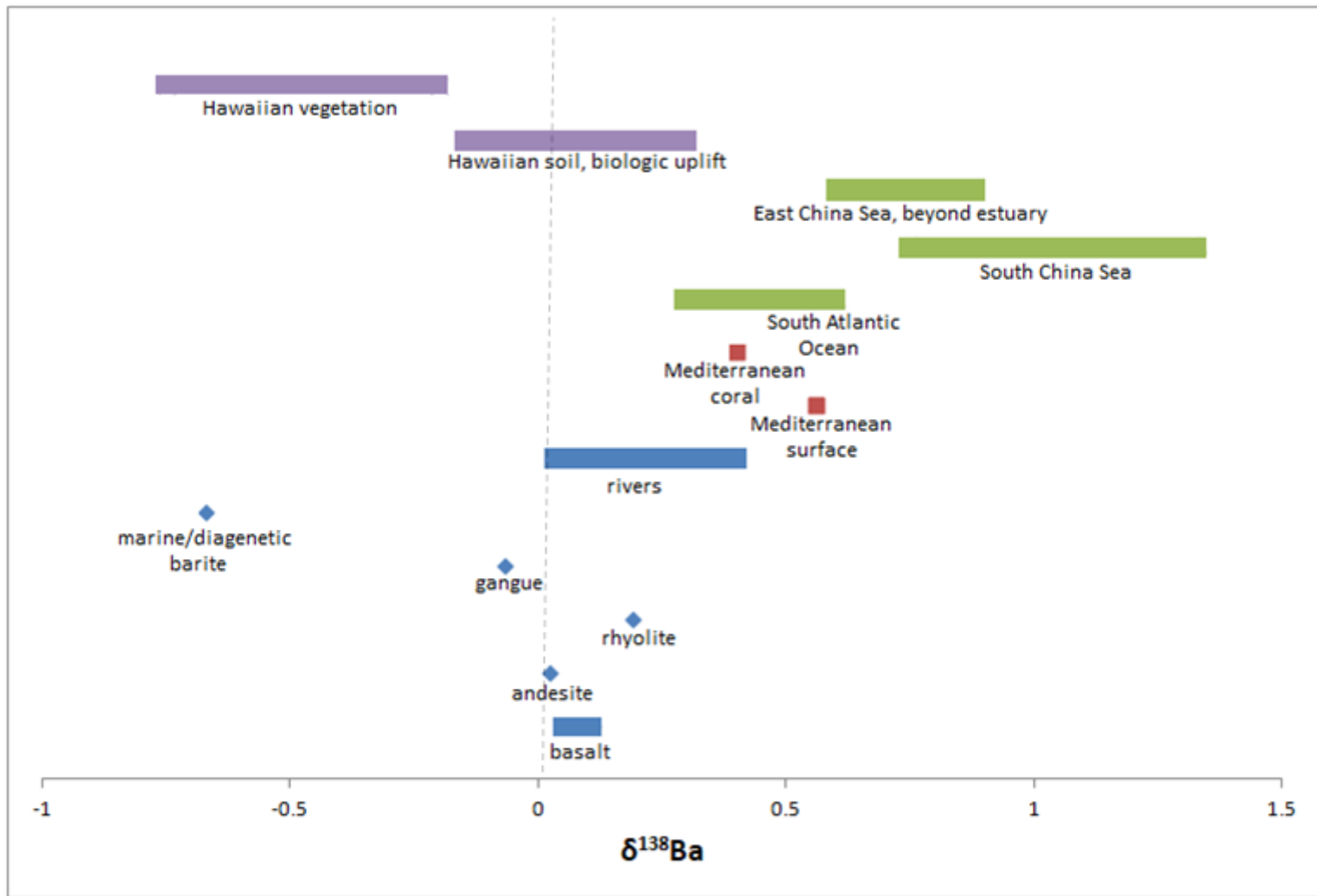


Figure 2: Overview of  $\delta^{138}\text{Ba}$  literature values (von Allmen et al., 2010; Bullen and Chadwick, 2015; Cao et al., 2015; Horner et al., 2015; Nian et al., 2015; Pretet et al., 2015)

### **1.3.4 Ba isotope variations in igneous rock and river water**

Barium isotope studies of igneous rocks have been limited primarily to standard materials, and the total range of  $\delta^{138}\text{Ba}$  values found to date is -0.2‰ to 0.2‰ (Miyazaki et al., 2014; Bullen and Chadwick, 2015; Nan et al., 2015). Miyazaki et al. (2014) found a total  $\delta^{138}\text{Ba}$  range in andesite and basalt standards of <0.1‰. Tephra and lava found in Hawaii (~650-1200 ppm) showed minor Ba isotope fractionation, ranging from  $\delta^{138}\text{Ba}$  values of -0.02‰ to 0.10‰ (Bullen and Chadwick, 2015). Nan et al. (2015) found that most igneous rock standards yielded  $\delta^{138}\text{Ba}$  values in the range of 0.0-0.1‰, but one rhyolite reached 0.19‰, and a late Mesozoic basalt from China yielded a low value of -0.18‰. Terrestrial gangue (commercially unwanted material that surrounds or is mixed with ore, in this case barite and double carbonate) from Germany and Namibia hovered between  $\delta^{138}\text{Ba}$  -0.13 and 0.00‰ (von Allmen et al., 2010) relative to standard IAEA-CO-9, which is essentially within error of NIST 3104a (Nan et al., 2015).

$\delta^{138}\text{Ba}$  values from selected rivers around the world are reported by Cao et al. (2016). The Changjiang, Amazon, and Yukon rivers have  $\delta^{138}\text{Ba}$  values from 0.0 to 0.13‰, while the Pearl, Sepik and Danube Rivers yield values of about 0.15 to 0.27‰. The Lena and Colorado Rivers reach values of 0.4‰. There is no apparent correlation with barium concentration, and the factors controlling the  $\delta^{138}\text{Ba}$  of river waters have not yet been determined.

### **1.3.5 Fractionation from biologically driven processes**

Bullen and Chadwick (2015) reported  $\delta^{138}\text{Ba}$  results from a study of Hawaiian parent rock, soil, and vegetation. They found that biological uplift, the pulling of nutrients from deeper in soils upward toward roots, creates stratification seen in both exchangeable sites and soil water. The barium near the surface was found to average around 0.10-0.15‰ lighter than the parent material (igneous rock,  $\delta^{138}\text{Ba} \approx 0.08\text{‰}$ ), while the soil exchange and soil water 25 cm down could be

0.15‰ to 0.35‰ heavier. The exchangeable fraction in the soil and soil water had very similar values throughout, but there was perhaps a slight preference for lighter barium in the exchangeable sites. The barium within the plant itself experienced extreme fractionation at the roots—0.75‰ lighter than the lava rock parent material—but this fractionation lessened up into the stem and neared again the numbers seen at the soil's surface within the foliage.

Pretet et al. (2016) cultured corals in a tank of known  $\delta^{138}\text{Ba}$  to study the fractionation that occurred in aragonite-structured witherite. Barium present as an impurity in coral aragonite is isotopically lighter than surrounding seawater by 0.12‰. They suggest that vital effects play an important role in the  $\delta^{138}\text{Ba}$  of the coral, rather than simple equilibration between the coral and ambient seawater.

Dissolved barium follows a concentration gradient similar to nutrients in the oceanic water column, most likely due the formation of barite due to biological processes (Horner, et al., 2015) and adsorption of barium onto biogenic particles (Cao, et al., 2015). There is a definite correlation between concentration of barium and extent of isotope fractionation (Horner et al., 2015; Figure 3). Surface water in the south Atlantic (0.92° E, 39.99° S) show  $\delta^{138}\text{Ba}$  values of 0.6‰, which drop in a linear fashion to below 0.4‰ starting around 1500 m depth, and stabilizes there until 3000 m before dropping again to 0.3‰ at 4000 m (Horner, et al., 2015).

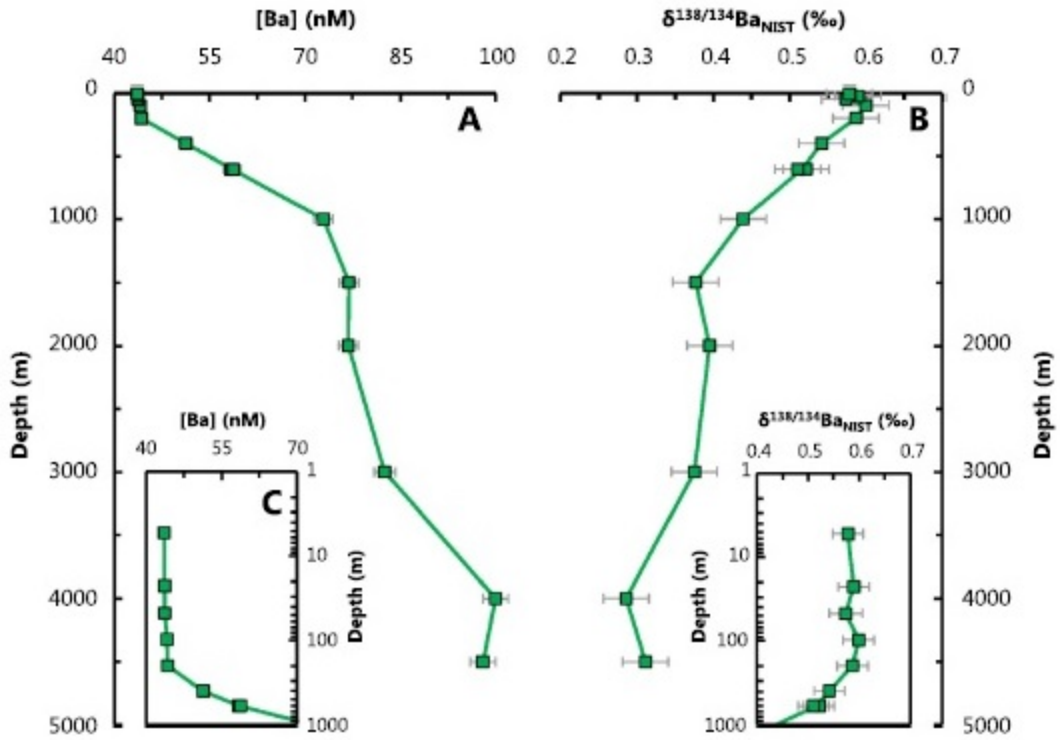


Figure 3: Trend of barium concentration and  $\delta^{138}\text{Ba}$  with ocean depth, southern Atlantic Ocean, 39.99° S, 0.92° E (modified from Horner et al., 2015)

Cao et al. (2016) studied barium fractionation throughout the water column in several areas of the East and South China Seas. In most areas, the surface values were high, with  $\delta^{138}\text{Ba} \approx 1.3\text{‰}$ . The drop in  $\delta^{138}\text{Ba}$  with increased depth was similar to that seen in the southern Atlantic. The  $\delta^{138}\text{Ba}$  decreased in a regular fashion until a depth of 1000 m. From there to the bottom of the recorded area (below 3500 m), values remained around 0.70—0.80‰. One study area, however, was quite different. A station in the East China Sea just beyond the Changjiang river estuary had a much lower  $\delta^{138}\text{Ba}$  of 0.40‰ with an extremely high concentration of barium:  $175 \text{ nm kg}^{-1}$  as opposed to the average  $<45$  seen in other stations in the area. The  $\delta^{138}\text{Ba}$  rapidly increased with depth as the barium concentration decreased, the opposite of what was seen in the Atlantic and in even the other areas studied by Cao et al. (2016). This could be due to the influence of riverine input of Ba at this site.

The only known sample of marine and diagenetic barite is very light isotopically, around  $\delta^{138}\text{Ba} \approx -0.7\text{‰}$  in the Demerara Rise, an offshore section of South America in the equatorial Atlantic (von Allmen et al., 2010).

### **1.3.6 Ba isotope fractionation from other processes**

Barium diffusion experiments in which a  $\text{BaCl}_2$  solution diffused through silica hydrogel (van Zuilen et al., 2016) resulted in significant fractionation, in which the diffusing species was lighter than the starting solution by up to 2.9‰. These results could be explained by a diffusion-transport model in which the isotopes of Ba exhibited mass-dependent variations in diffusivity. Adsorption of Ba onto the surface of the silica gel favored the heavier isotope, but the effect was significantly smaller than that resulting from diffusion.

## **2.0 BARIUM ISOTOPE METHOD DEVELOPMENT**

### **2.1 OVERVIEW OF BA ISOTOPE MEASUREMENT METHODOLOGY AND REQUIREMENTS**

The measurement of barium isotopes is a multi-step process. In order to measure the barium in a substance, the barium must be removed from its matrix, which involves converting it into a solution with sufficient barium concentration and processing it through cation exchange resin to eliminate the other elements in the matrix. In some cases, additional chemistry or calibrations must be done when matrix or residue has unwanted reactions with the resin. The separation chemistry and measurement on the MC-ICP-MS can cause additional fractionation, often significantly larger than the natural variations in the samples. To adjust for this, an isotopic double spike of precisely-known composition is added to the sample before any chemical processing that could cause fractionation.

### **2.2 CATION EXCHANGE COLUMN SEPARATION OF BA**

#### **2.2.1 Sample preparation**

In order to obtain precise measurement of the Ba isotope ratio, it is necessary to remove elements other than Ba from the matrix because (1) some elements have isotopes with isobaric interferences on one or more Ba isotopes, and (2) excess cations in the solution can cause non-

linear fractionation effects during measurement on the MC-ICP-MS that are not replicated by the standards. To this end, the samples need to be prepared for purification via cation exchange. In order to obtain at least 2 mL of a 500  $\mu\text{g/L}$  solution of Ba for MC-ICPS analysis, each sample required at least one microgram of barium; however, 2.5  $\mu\text{g}$  or more was generally prepared so that multiple measurements could be made. For the produced water samples, preparation was relatively simple: the concentration of barium was measured via ICP-MS, the appropriate amount was aliquoted, double spike was added, and the sample was evaporated to dryness. For the core samples, sequential extraction removed the portions to be measured, the concentration of Ba in leachates was determined, and the leachates were aliquoted, spiked, and evaporated to dryness.

One mL of concentrated hydrochloric acid (HCl) was added to the dried, spiked samples, the sample was dried again to convert the matrix to chloride form, and then 0.5 mL of 2.0 N HCl was added to redissolve the sample. Each time acid was added to the dried sample it was sonicated for five minutes and allowed to equilibrate for at least 30 minutes.

### **2.2.2 Columns and cation exchange resin**

The cation column separation chemistry developed in this study is based on techniques described by von Allmen et al. (2010), Miyazaki et al. (2014), Horner et al. (2015), Nan et al. (2015), and Bullen and Chadwick (2015). A detailed, step-by-step description of the procedure is provided in the Appendix. Teflon columns (manufactured by Savillex<sup>®</sup>) with an interior diameter of 4.8 mm, a height of 7.5 mm, and a 15 mL reservoir were filled to just below the base of the reservoir (6 cm resin height above the frit) with AG-50W, 200-400 mesh, 8% cross-linkage cation exchange resin suspended in 2.0 N HCl.

The resin is pre-cleaned by placing it in a Teflon bottle, which is filled with a series of cleaning solutions and shaken vigorously, then allowed to sit for five minutes (except where noted) before the fluid is carefully decanted. The solutions used were in the following sequence: Milli-Q ultrapure (18.2 MΩ) water (four rinses); 2% ultrapure HNO<sub>3</sub> (twice), Milli-Q water (twice), 6 N ultrapure HCl (allowed to sit 2-3 hours); Milli-Q water; 6 N ultrapure HCl; and finally Milli-Q water twice more or until the decanted water is clear in color, whichever comes last. The resin is stored in Milli-Q water.

After the cation exchange resin is added to the columns, it is conditioned with 0.5 mL of 4.0 N HCl, followed by 2 mL of 4.0 N HCl, then 4 mL of the same. This was repeated with 2.0 N HCl. The resin is discarded from the column after each sample passes through.

### **2.2.3 Column calibration**

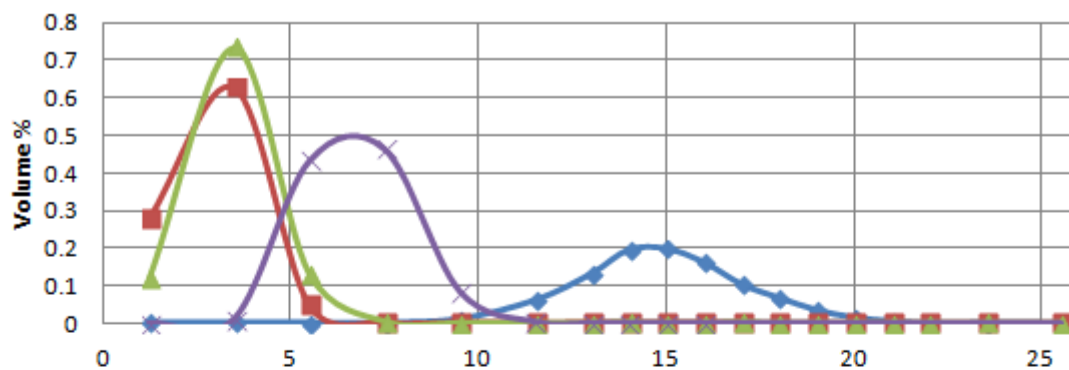
Cations move through the resin at a rate determined by their size, charge, and complexation with H<sub>2</sub>O and Cl<sup>-</sup>. The goal is to find an elution curve that best separates Ba<sup>2+</sup> from all other cations. Initial column calibrations were carried out using produced water samples of approximately known chemistry and were occasionally spiked with a concentrated solution of rare earth elements (REEs) to test the separation of barium from lanthanum (La) and cerium (Ce), which have isobaric interferences with <sup>136</sup>Ba (<sup>136</sup>La) and <sup>138</sup>Ba (<sup>138</sup>La, <sup>138</sup>Ce).

**2.2.3.1 Produced water calibration curves** The elution of produced water was first attempted with 2.0 N HCl only (Bullen and Chadwick, 2015, Horner, et al., 2015), and different resin heights were tested to determine the best separation of Ba from the matrix. While major cations like Na<sup>+</sup> and Mg<sup>2+</sup> were eluted quickly (within the first ~12 mL), Sr<sup>2+</sup> tended to overlap with Ba<sup>2+</sup> at lower resin heights (Figure 4); ultimately, a 6 cm height was chosen as optimal. A relatively clean separate of Ba was eluted between 15 and 25 mL total acid added. Using 2.0 N

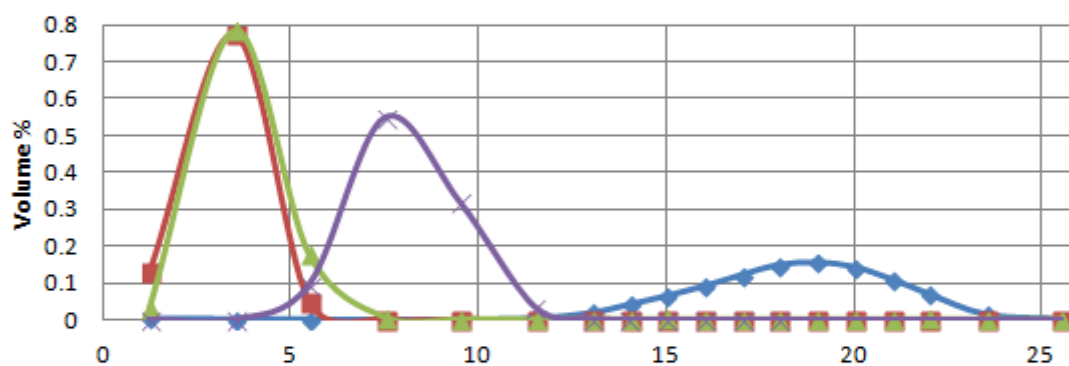
HCl only, most of the major cations were removed within the first 15 mL, and  $\text{Ce}^{3+}$  and  $\text{La}^{3+}$  were not significantly eluted until after 25 mL, subsequent to the elution of  $\text{Ba}^{2+}$  (Figure 5). In order to accelerate the Ba collection process and reduce the amount of acid used, we tried experiments in which the Ba fraction was collected using 4.0 N HCl, 1.0 N  $\text{HNO}_3$ , and 1.5 N  $\text{HNO}_3$  (after Miyazaki et al., 2014, and Horner et al., 2015). As shown in Figure 6, all of these resulted in increased overlap of  $\text{Ce}^{3+}$  and  $\text{La}^{3+}$  with  $\text{Ba}^{2+}$ ; therefore, the initial elution using 2.0 N HCl all the way through was used in this study.

**2.2.3.2 Sequential extraction calibration curves** Elution curves for Ba and other elements were found to be different in the ammonium acetate and acetic acid sequential extractions of shale, most likely due to interference between the column chemistry and residual acetate from the extraction solutions. As noted earlier, Ba in produced waters was eluted between 15 and 25 mL of 2.0 N HCl. When this elution interval was with the products of sequential extraction, only about half of the Ba was eluted by 25 mL; the remainder came out in the next ~10 mL of 2.0 N HCl. Therefore, a second separation was done on these samples. In the first separation, the 16-38 mL fraction was collected, evaporated to dryness, and put through the columns again. In the second pass through the column, the 15-30 fraction was collected for analysis (Figure 7). While this had the effect of cutting off a portion of the Ba, the double-spike technique allows correction for mass fractionation from incomplete sample recovery, and we deemed it more important to minimize interferences with the analysis.

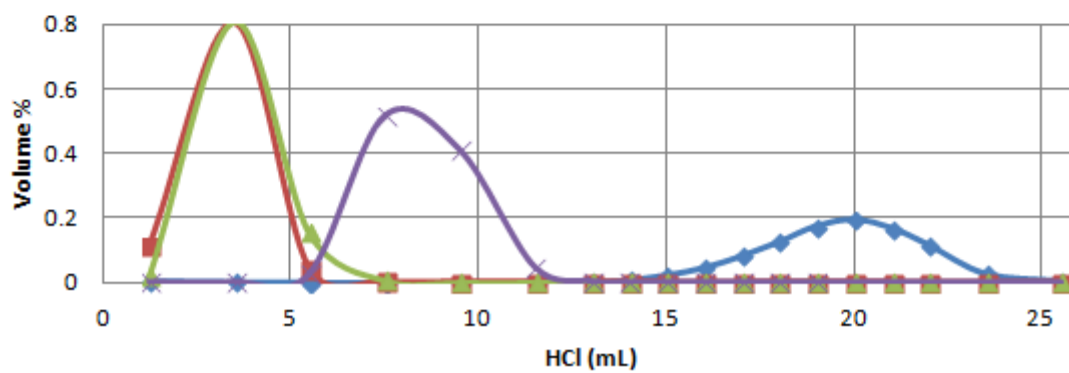
### 4 cm Resin



### 5 cm Resin



### 6 cm Resin



◆ Ba    ■ Na    ▲ Mg    × Sr

Figure 4: Cation separation using different resin heights

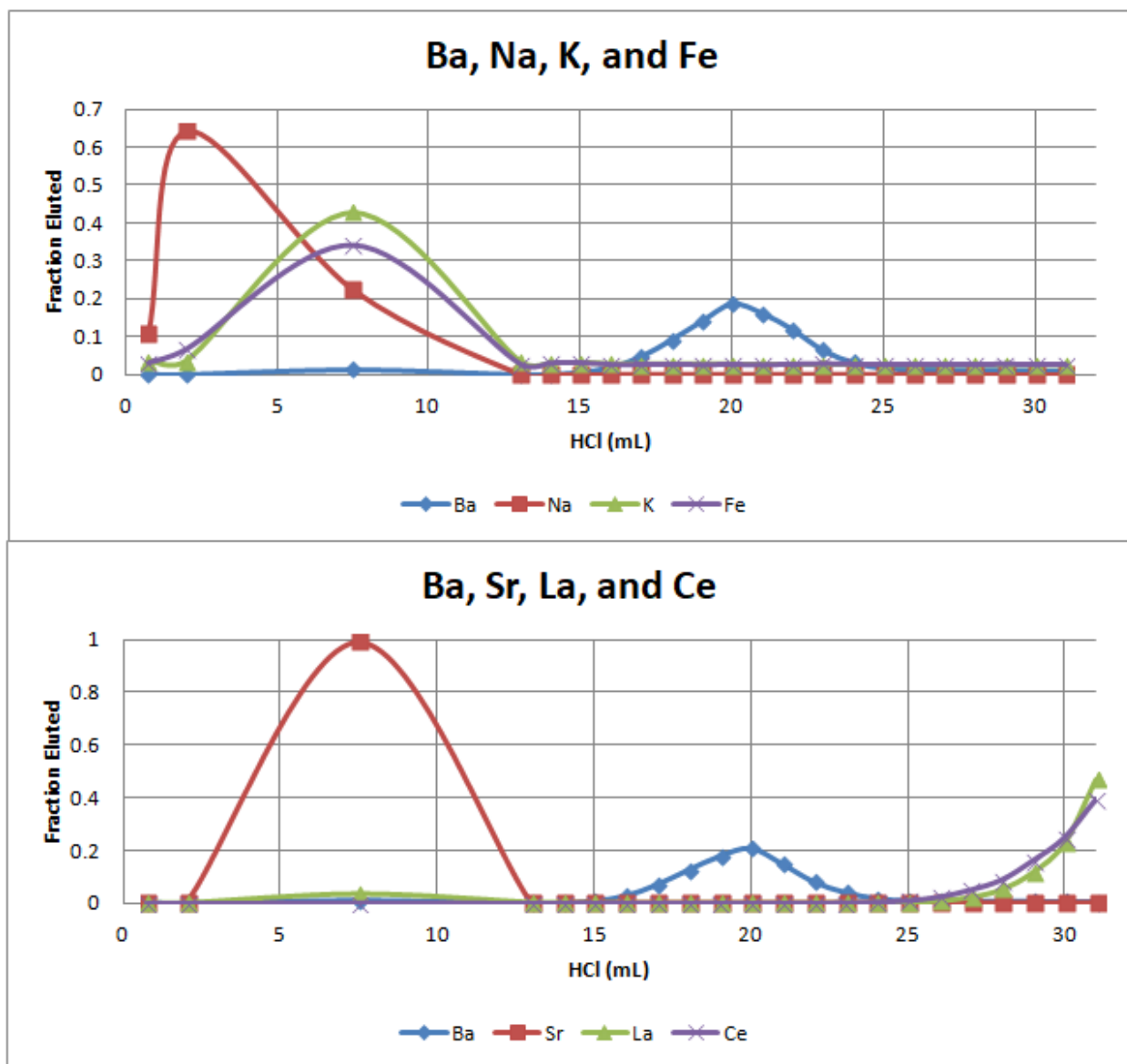


Figure 5: Final produced water elution curve of Ba, major elements, and potential REE isobaric interferences (La and Ce) using 6 cm resin heights

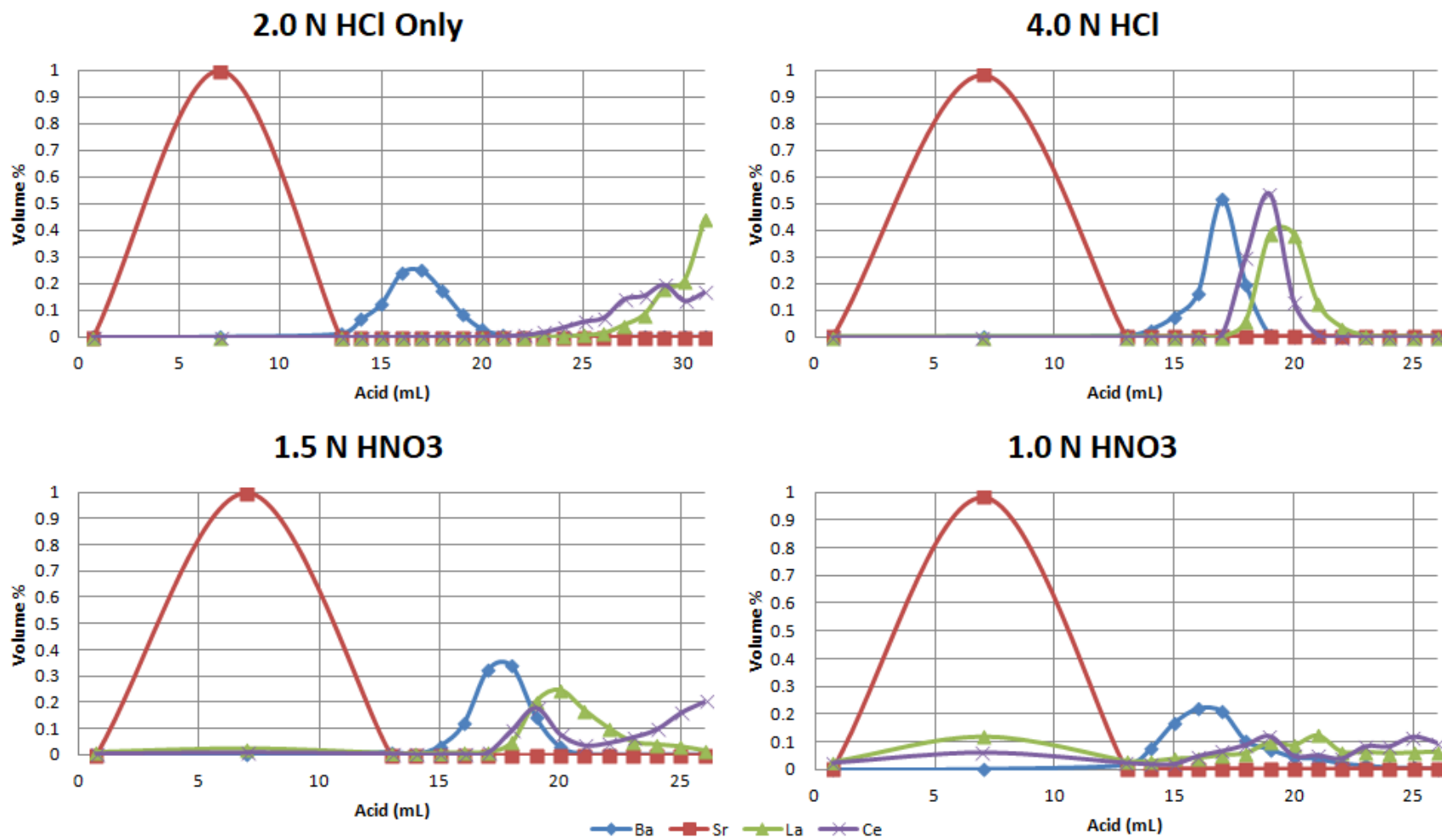


Figure 6: Elution curves of selected elements in produced waters using different acids after the first 13.5 mL of 2.0 N HCl were added.

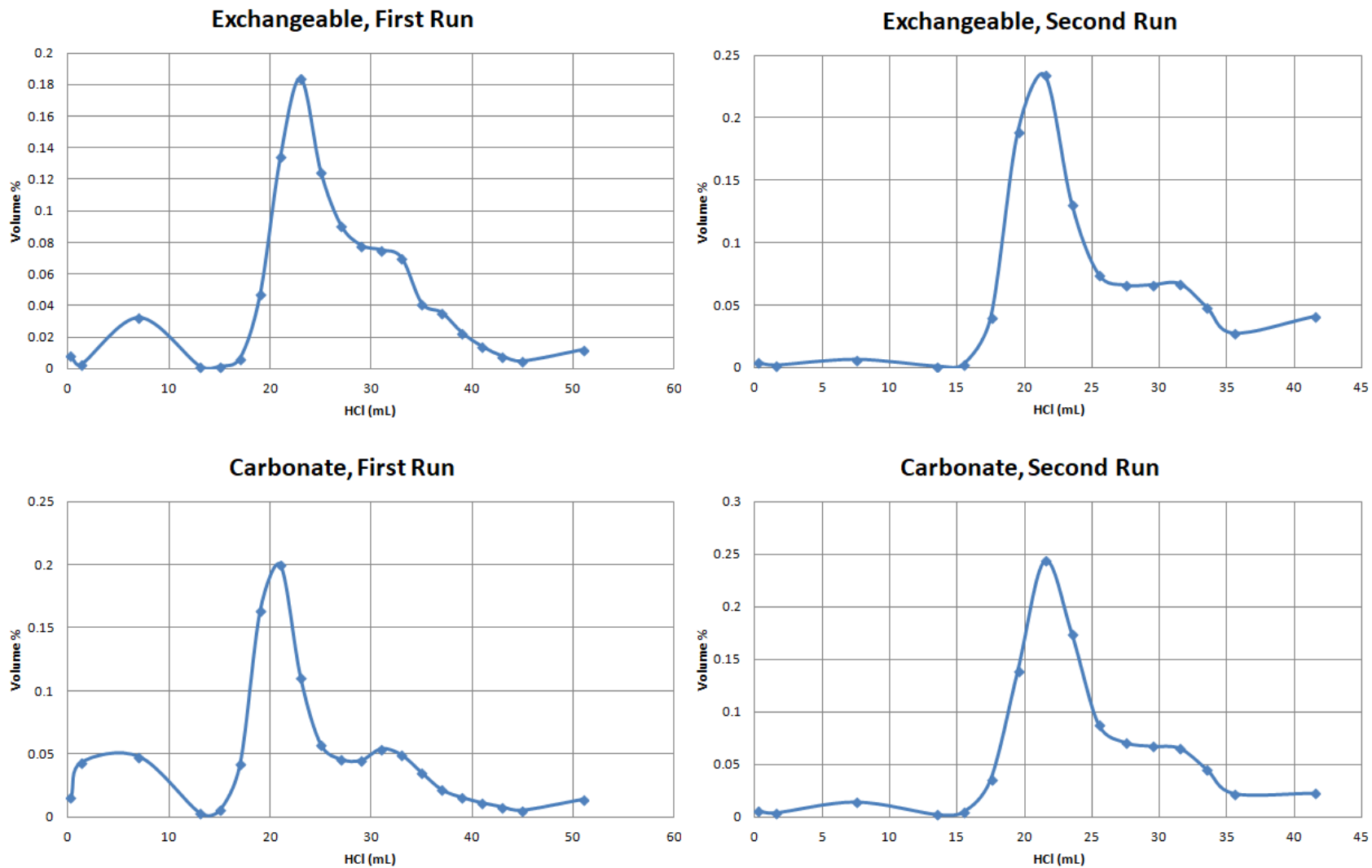


Figure 7: First and second elutions of sequentially extracted barium. In the second run, Ba from the first column (15-38 mL) was put through a second column with new resin.

## 2.3 BARIUM DOUBLE SPIKE

### 2.3.1 Theory

Using a double spike to correct for instrumental mass fractionation is a long-established technique (Dodson, 1963; Eugster et al., 1969). The process requires an element with at least four stable (or sufficiently stable) isotopes. A precisely-measured solution enriched in two of the isotopes is added to the sample. Knowing the relationship between the four chosen isotopes in the standard (NIST3104a in this study) allows fractionation between the two non-spiked isotopes that can occur during chemistry and instrumental measurement to be determined iteratively (Dodson, 1963; Rudge et al., 2009).

### 2.3.2 Choice of spike isotopes

The relatively large number of barium isotopes provides a variety of choices in creating a double spike. Creation of the double spike depended primarily on balancing the variables of isobaric interferences, natural isotope abundances, and availability of isotope spikes of sufficient purity. Of the isobaric interferences (Table 1), Xe presents the most serious issue, because some level of Xe is always present in the Ar gas used for sample introduction in the MC-ICP-MS. Meanwhile, Ce and La can be minimized by optimizing column chemistry. We chose not to analyze  $^{130}\text{Ba}$  and  $^{132}\text{Ba}$  due to their low abundances, and because  $^{132}\text{Ba}$  has the largest interference from Xe, and the potential tellurium (Te) interference in  $^{130}\text{Ba}$  could have caused additional difficulty. To determine between the final five possible isotopes, Rudge's Double Spike Toolbox (presented first in Rudge et al., 2009, and available on the author's website) was consulted to determine which isotopes would be used in the spike, which would be measured, and what the proper proportions would be.

Ultimately, a  $^{135}\text{Ba}$ - $^{137}\text{Ba}$  spike was chosen, as  $^{138}\text{Ba}$ , the most abundant isotope, could be measured together with either  $^{134}\text{Ba}$  or  $^{136}\text{Ba}$  (Figure 8). Between these, there was no change in calculated error and only minor changes to the optimal proportions of  $^{135}\text{Ba}/(^{135}\text{Ba}+^{137}\text{Ba})$  within the double spike depending on which isotope pair was chosen for measurement (0.669 for  $^{138}\text{Ba}/^{134}\text{Ba}$  versus 0.682 for  $^{138}\text{Ba}/^{136}\text{Ba}$ ; Figure 9). Similarly, the spike to sample proportion (40.32% spike for  $^{138}\text{Ba}/^{134}\text{Ba}$  versus 41.72% in  $^{138}\text{Ba}/^{136}\text{Ba}$ ; Figure 9) was very close, so a

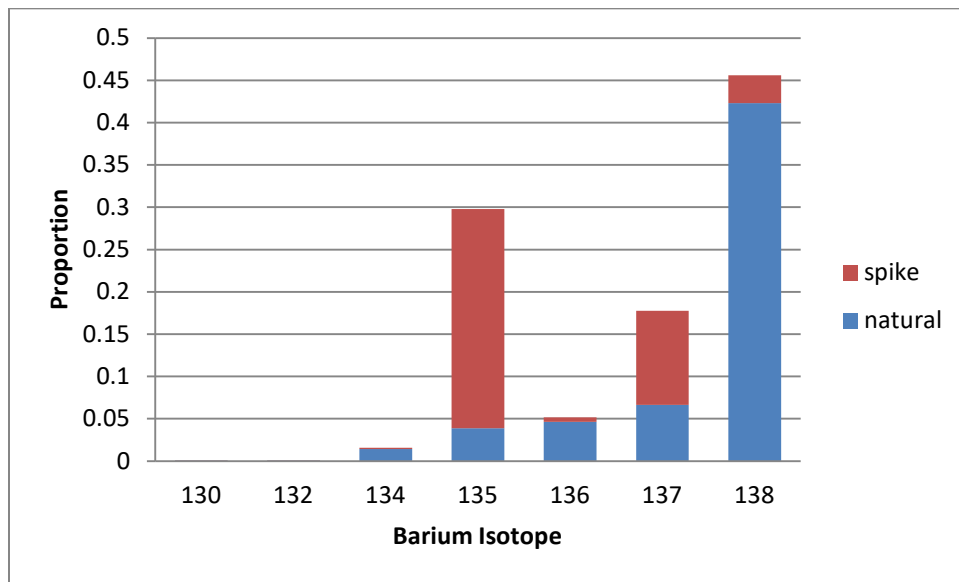


Figure 8: The isotope abundances of an optimally-spiked sample

Table 1: Abundances and isobaric interferences for barium and overlapping isotopes

	130	131	132	133	134	135	136	137	138	139	140	141	142
Ce							0.19		0.25		88.45		11.11
La									0.089	99.91			
<b>Ba</b>	<b>0.11</b>		<b>0.10</b>		<b>2.42</b>	<b>6.59</b>	<b>7.85</b>	<b>11.23</b>	<b>71.70</b>				
Xe	4.07	21.23	26.91		10.44		8.86						
Te	34.08												

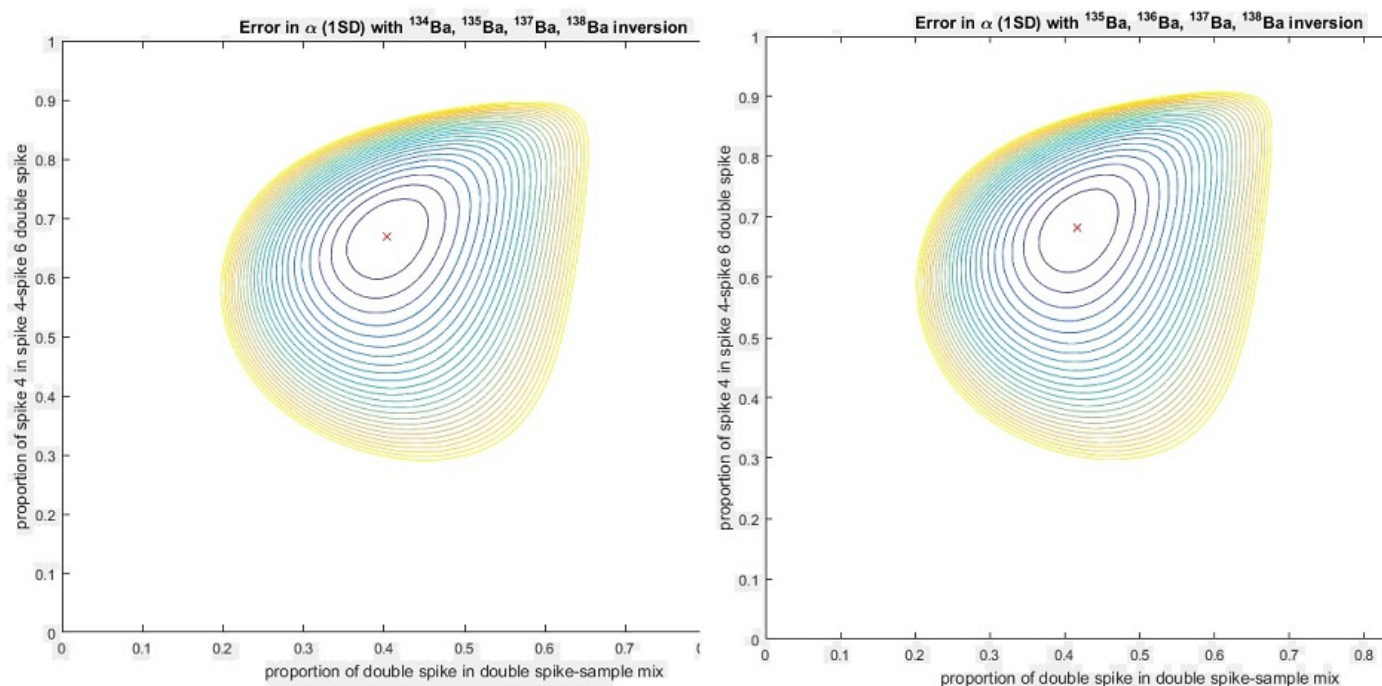


Figure 9: Error curves for the proportions of  $^{135}\text{Ba}$  (spike 4) and  $^{137}\text{Ba}$  (spike 6) and for the proportions of double spike and sample. Left is optimized for measurement of  $^{138}\text{Ba}/^{134}\text{Ba}$ ; right is optimized for measurement of  $^{138}\text{Ba}/^{136}\text{Ba}$ . Created using the double spike toolbox (Rudge et al., 2009; <http://www.johnrudge.com/doublespike>).

halfway point in each of the two sets of proportions was used in creating the spike and determining how much would be added to samples for measurement.

The sample-spike measurement configuration that we selected was the  $^{135}\text{Ba}$ - $^{137}\text{Ba}$  spike combined with the  $^{138}\text{Ba}$ - $^{136}\text{Ba}$  measurement to correct for mass fractionation.  $^{136}\text{Ba}$  was measured instead of  $^{134}\text{Ba}$  because (1)  $^{136}\text{Ba}$  is more abundant, and (2) the Xe interference on  $^{136}\text{Ba}$  is smaller than that on  $^{134}\text{Ba}$  (Table 1). While  $^{136}\text{Ba}$  has a small Ce interference that is not present on  $^{134}\text{Ba}$ , Ce is effectively removed during column separations, and later measurements showed the interference to be negligible on all samples. The  $^{138}\text{Ba}/^{134}\text{Ba}$  ratio (used to report  $\delta^{138}\text{Ba}$ ) is calculated based on the measured  $^{138}\text{Ba}/^{136}\text{Ba}$  ratio.

### 2.3.3 Calculating sample $^{138}\text{Ba}/^{134}\text{Ba}$ from isotope ratio measurements

Eight isotope masses are measured on the MC-ICPMS during a Ba isotope run: 131, 134, 135, 136, 137, 138, 139, and 140. Of these, mass 131 is used to monitor  $^{131}\text{Xe}$ , mass 139 to monitor  $^{139}\text{La}$ , mass 140 to monitor  $^{140}\text{Ce}$ , and mass 134 (primarily  $^{134}\text{Ba}$ ) is not used directly to determine the  $\delta^{138}\text{Ba}$  value. The other four isotopes are used, after appropriate corrections for isobaric interferences, to calculate the  $\delta^{138}\text{Ba}$  of the sample. An exponential correction was used to correct for mass fractionation, as

$$\frac{^{138}\text{Ba}}{^{136}\text{Ba}}_{\text{corrected}} = \frac{^{138}\text{Ba}}{^{136}\text{Ba}}_{\text{measured}} \left( \frac{m_{138}}{m_{136}} \right)^{\alpha m_{136}}$$

where  $m_{138}$  and  $m_{136}$  are the isotope masses of  $^{138}\text{Ba}$  and  $^{136}\text{Ba}$  (137.90523 and 135.904553 amu, respectively) and  $\alpha$  is the exponential fractionation factor, given by:

$$\alpha = \ln \left( \frac{\left( \frac{^{138}\text{Ba}}{^{136}\text{Ba}} \right)_N / \left( \frac{^{138}\text{Ba}}{^{136}\text{Ba}} \right)_M}{m_{136} \times \ln(m_{138}/m_{136})} \right)$$

(Wasserburg et al., 1981). Here  $(^{138}\text{Ba}/^{136}\text{Ba})_N$  refers to the “normal” value for unfractionated barium (in this case, the value of standard NIST 3104a) and  $(^{138}\text{Ba}/^{136}\text{Ba})_M$  is the measured value. The value of  $\alpha$  calculated above can be used to correct all isotope ratios with  $^{136}\text{Ba}$  in the denominator.

When the double spike is added to the sample, it has a fractionation factor,  $\alpha_{\text{spike}}$ , of zero (by definition). Therefore, the goal is find the value of  $\alpha_{\text{spike}}$  after chemistry and analysis, and to use that to correct for post-spiking mass fractionation. This allows calculation of the sample fractionation prior to spiking as  $\alpha_{\text{sample}}$ . An iterative sequence of calculations to correct for mass fractionation is as follows:

1. Calculate spike to sample ratio as  $^{135}\text{Ba}_{\text{spike}}/^{136}\text{Ba}_{\text{sample}}$  as a function of:
  - a.  $(^{135}\text{Ba}/^{136}\text{Ba})_{\text{measured}}$  (original measured value)
  - b.  $(^{135}\text{Ba}/^{136}\text{Ba})_{\text{sample}}$  (from previous 4)
  - c.  $(^{135}\text{Ba}/^{136}\text{Ba})_{\text{spike}}$  (from previous 8)
  
2. Calculate  $(^{138}\text{Ba}/^{136}\text{Ba})_{\text{sample}}$  as a function of:
  - a.  $(^{138}\text{Ba}/^{136}\text{Ba})_{\text{measured}}$  (original measured value)

- b.  $^{135}\text{Ba}_{\text{spike}}/^{136}\text{Ba}_{\text{sample}}$  (from 1)
- c.  $(^{135}\text{Ba}/^{136}\text{Ba})_{\text{spike}}$  (from previous 8)
- d.  $(^{138}\text{Ba}/^{136}\text{Ba})_{\text{spike}}$  (from previous 9)
3. Calculate  $\alpha_{\text{sample}}$  as a function of:
- a.  $(^{138}\text{Ba}/^{136}\text{Ba})_{\text{sample}}$  (from 2)
- b.  $(^{138}\text{Ba}/^{136}\text{Ba})_{\text{normal}}$  (constant)
- c. Masses of  $^{138}\text{Ba}$ ,  $^{136}\text{Ba}$  (constants)
4. Calculate  $(^{135}\text{Ba}/^{136}\text{Ba})_{\text{sample}}$  as a function of:
- a.  $\alpha_{\text{sample}}$  (from 3)
- b.  $(^{138}\text{Ba}/^{136}\text{Ba})_{\text{normal}}$  (constant)
- c. Masses of  $^{135}\text{Ba}$ ,  $^{136}\text{Ba}$  (constants)
5. Calculate  $(^{137}\text{Ba}/^{136}\text{Ba})_{\text{sample}}$  as a function of:
- a.  $\alpha_{\text{sample}}$  (from 3)
- b.  $(^{137}\text{Ba}/^{136}\text{Ba})_{\text{normal}}$  (constant)
- c. Masses of  $^{137}\text{Ba}$ ,  $^{136}\text{Ba}$  (constants)
6. Calculate  $(^{137}\text{Ba}/^{135}\text{Ba})_{\text{spike}}$  as a function of:
- a.  $(^{137}\text{Ba}/^{136}\text{Ba})_{\text{measured}}$  (original measured value)
- b.  $(^{135}\text{Ba}/^{136}\text{Ba})_{\text{measured}}$  (original measured value)
- c.  $(^{135}\text{Ba}/^{136}\text{Ba})_{\text{sample}}$  (from 4)

d.  $^{135}\text{Ba}_{\text{spike}}/^{136}\text{Ba}_{\text{sample}}$  (from 1)

e.  $(^{137}\text{Ba}/^{136}\text{Ba})_{\text{sample}}$  (from 5)

7. Calculate  $\alpha_{\text{spike}}$  as a function of:

a.  $(^{137}\text{Ba}/^{135}\text{Ba})_{\text{spike}}$  (from 6)

b.  $(^{137}\text{Ba}/^{136}\text{Ba})_{\text{SpikeNormal}}$  (constant)

c.  $(^{135}\text{Ba}/^{136}\text{Ba})_{\text{SpikeNormal}}$  (constant)

d. Masses of  $^{137}\text{Ba}$ ,  $^{135}\text{Ba}$  (constants)

8. Calculate  $(^{135}\text{Ba}/^{136}\text{Ba})_{\text{spike}}$  as a function of:

a.  $\alpha_{\text{spike}}$  (from 7)

b.  $(^{135}\text{Ba}/^{136}\text{Ba})_{\text{SpikeNormal}}$  (constant)

c. Masses of  $^{135}\text{Ba}$ ,  $^{136}\text{Ba}$  (constants)

9. Calculate  $(^{138}\text{Ba}/^{136}\text{Ba})_{\text{spike}}$  as a function of:

a.  $\alpha_{\text{spike}}$  (from 7)

b.  $(^{138}\text{Ba}/^{136}\text{Ba})_{\text{SpikeNormal}}$  (constant)

c. Masses of  $^{138}\text{Ba}$ ,  $^{136}\text{Ba}$  (constants)

10. REPEAT

In the first iteration, the standard (NIST 3104a) ratio is used for ratio 1.b., and unfractionated spike ratios are used for 1.c., 2.c., and 2.d.. Thereafter, the values from the

previous set of iterations are used. The values typically converge after 2-3 iterations, but 10 full iterations are done for each measured set of ratios. Ultimately  $\alpha_{\text{sample}}$  (Step 3) is used to calculate the final  $(^{134}\text{Ba}/^{136}\text{Ba})_{\text{sample}}$ , which is then converted to  $(^{138}\text{Ba}/^{134}\text{Ba})_{\text{sample}}$  as

$$(^{138}\text{Ba}/^{134}\text{Ba})_{\text{sample}} = (^{138}\text{Ba}/^{136}\text{Ba})_{\text{sample}} / (^{134}\text{Ba}/^{136}\text{Ba})_{\text{sample}}$$

The iterative calculations were tested by numerically fractionating a “sample,” numerically mixing it with unfractionated spike, and numerically fractionating the mixture using the exponential law. The isotope ratios of the fractionated mixture were run through the iteration program, and the precise initial composition of the “sample” was obtained. This held for all spike:sample ratios, and for extreme values of  $\alpha$  (positive or negative).

While the exponential law has been shown to be effective in correcting for fractionation during sample chemistry and analysis by thermal ionization mass spectrometry (*e.g.*, Russell et al., 1978), some portion of the fractionation during MC-ICP-MS results from processes (possibly related to sample introduction in the plasma) that do not follow an exponential law. Therefore, it is necessary to measure a spiked standard (in this case, NIST 3104a) repeatedly throughout the analysis, and to normalize the double spike-corrected values to this standard.

## 2.4 ANALYSIS BY MC-ICP-MS

### 2.4.1 Run parameters

Sample solutions containing 500  $\mu\text{g/L}$  Ba in 2%  $\text{HNO}_3$  were analyzed on the NETL/University of Pittsburgh Thermo Neptune Plus MC-ICP-MS. The initial batch of samples was run using a quartz glass spray chamber, yielding  $^{138}\text{Ba}$  signals of 2-7 V ( $10^{-11}$   $\Omega$  resistor). A series of measurements was made on unspiked standard NIST 3104a and on the double spike solution before and after the sample analyses; the average of these values was used as the “normal” ratios

for samples analyzed during that series of measurements. An optimally-spiked solution of NIST 3104a was analyzed before and after each sample as well, to test for drift over the course of the analyses (total time 24-60 hours). For each analysis, 50 sets of ratios (i.e., 50 sets of measured masses 131, 134, 135, 136, 137, 138, 139 and 140) were obtained; the reported uncertainty is two times the standard error (2 S.E.) of these measurements, and is typically in the range of 0.042-0.070‰ (average uncertainty  $\pm 0.052\%$  2 S.E.). The measured values for the spiked standard over the initial set of analyses are shown in Figure 10a. The samples (produced waters) analyzed during this time were normalized to the average value of all the standards.

The second batch of samples was analyzed using the Apex<sup>®</sup> heated/cooled chamber sample introduction system, resulting in signals up to 20 V. Unspiked standards, double spike, and spiked standards were all measured as before, and the samples were again normalized to the average of the spiked standards. The variation in the spiked NIST 3104a standards is shown in Figure 10b. Uncertainties in the spiked standard analyses ranged from 0.025 to 0.049‰, with an average of  $\pm 0.036\%$  2 S.E.

#### **2.4.2 Isobaric interference corrections**

A small but steady signal of  $^{131}\text{Xe}$  was observed throughout the analyses. For the second batch of samples, the Xe interference with  $^{136}\text{Ba}$  was corrected by measuring the signal intensity at mass 131 and subtracting the calculated  $^{136}\text{Xe}$  (based on  $^{136}\text{Xe}/^{131}\text{Xe} = 0.417$ ) from the total signal intensity at mass 136. Because the Xe signal was constant, the total correction depended on the intensity of the sample signal. The calculated Xe corrections to the  $\delta^{138}\text{Ba}$  ranged from 0.07‰ to 0.69‰, with an average correction of 0.12‰. For the first batch of samples, Xe was corrected by subtracting the full background for each mass, and assuming that the Xe signal was constant over the run. Reproducibility of the standard runs indicates that this was a reasonable assumption,

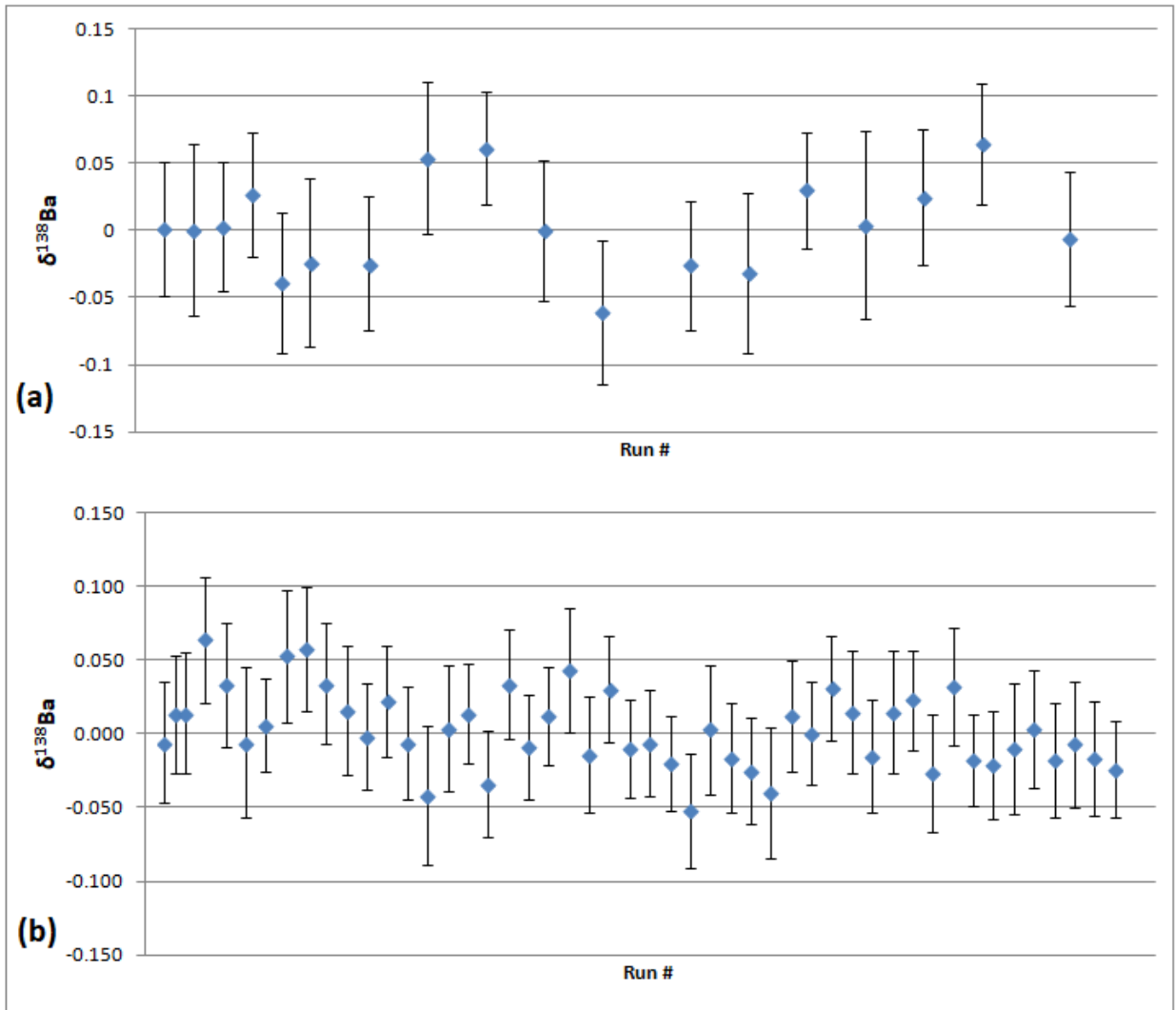


Figure 10: Measurements of standard during MC-ICP-MS runs; (a) initial runs (b) with Apex introduction system

although the lack of in-run Xe correction could be partly responsible for the larger uncertainty in the first batch of samples.

Possible interference from  $^{138}\text{La}$ ,  $^{136}\text{Ce}$ , and  $^{138}\text{Ce}$  were monitored at masses 139 ( $^{138}\text{La}/^{139}\text{La} = 0.00091$ ) and 140 ( $^{136}\text{Ce}/^{140}\text{Ce} = 0.0021$ ;  $^{138}\text{Ce}/^{140}\text{Ce} = 0.0028$ ). As expected, the total correction for all samples and standards was negligible (largest correction from  $^{138}\text{La} = 0.014\%$ ; most  $<0.001\%$ ); this is due to the efficient Ba separation chemistry and the relatively low abundance of the interfering isotopes.

### 2.4.3 Data evaluation

In addition to repeated runs of the spiked standard, nearly all samples were run in duplicate. In each case, the duplicates were within measurement uncertainty of the previous run. The factor that appeared to have the largest impact on measurement uncertainty was the overall intensity of the signal. In some cases, less sample than the optimal amount was available for analysis, leading to larger overall measurement uncertainty (up to  $\pm 0.12\%$  2 S.E.; Chapter 3). Smaller sample signals are correlated with higher Xe corrections, which may contribute to the higher uncertainty. If less Ba was present in the sample than expected prior to adding spike, the spike:sample ratio can also be elevated, which could contribute to the uncertainty. Accurate measurement of Ba concentrations in a sample prior to spiking is important for obtaining the best possible isotope data.

### **3.0 BARIUM ISOTOPE VARIATIONS IN THE MARCELLUS SHALE AND APPALACHAIN BASIN PRODUCED WATERS**

#### **3.1 INTRODUCTION**

The Marcellus Shale is the largest natural gas play in the United States, covering an area of 240,000 km<sup>2</sup> (Figure 11) and containing as much as 489 trillion cubic feet of recoverable natural gas (Kargbo et al., 2010). Around 4,000 unconventional wells were drilled into it between 2005 and 2014 in Pennsylvania alone (Balashov et al., 2015), and more than 240,000 people in the state are employed in the natural gas or related industry (MSC, 2013). Natural gas is extracted from the Marcellus Shale through a combination of directional drilling and hydraulic fracturing (Zagorski et al., 2012). Hydraulic fracturing involves injection of up to 15,000 m<sup>3</sup> of fluid (Ground Water Protection Council and ALL Consulting, 2009), consisting primarily of water (including fresh and/or previously returned water) with smaller amounts of sand proppant, acid for dissolving well casing perforations, and various chemical descalants (Soeder et al., 2014). The water is injected at high pressure to fracture the shale formation, creating permeability for gas flow. Following a waiting period after injection (sometimes referred to as “marinating”), the well is unsealed, and up to 40% of the water is returned to the surface, most of it within the first 1-2 weeks (Zagorski et al., 2012). During this time, the TDS (including Ba) of the returned water increases rapidly until it reaches a near-steady state value at a much-diminished flow rate (Hayes, 2009; Chapman et al., 2012; Kolesar Kohl et al., 2014).

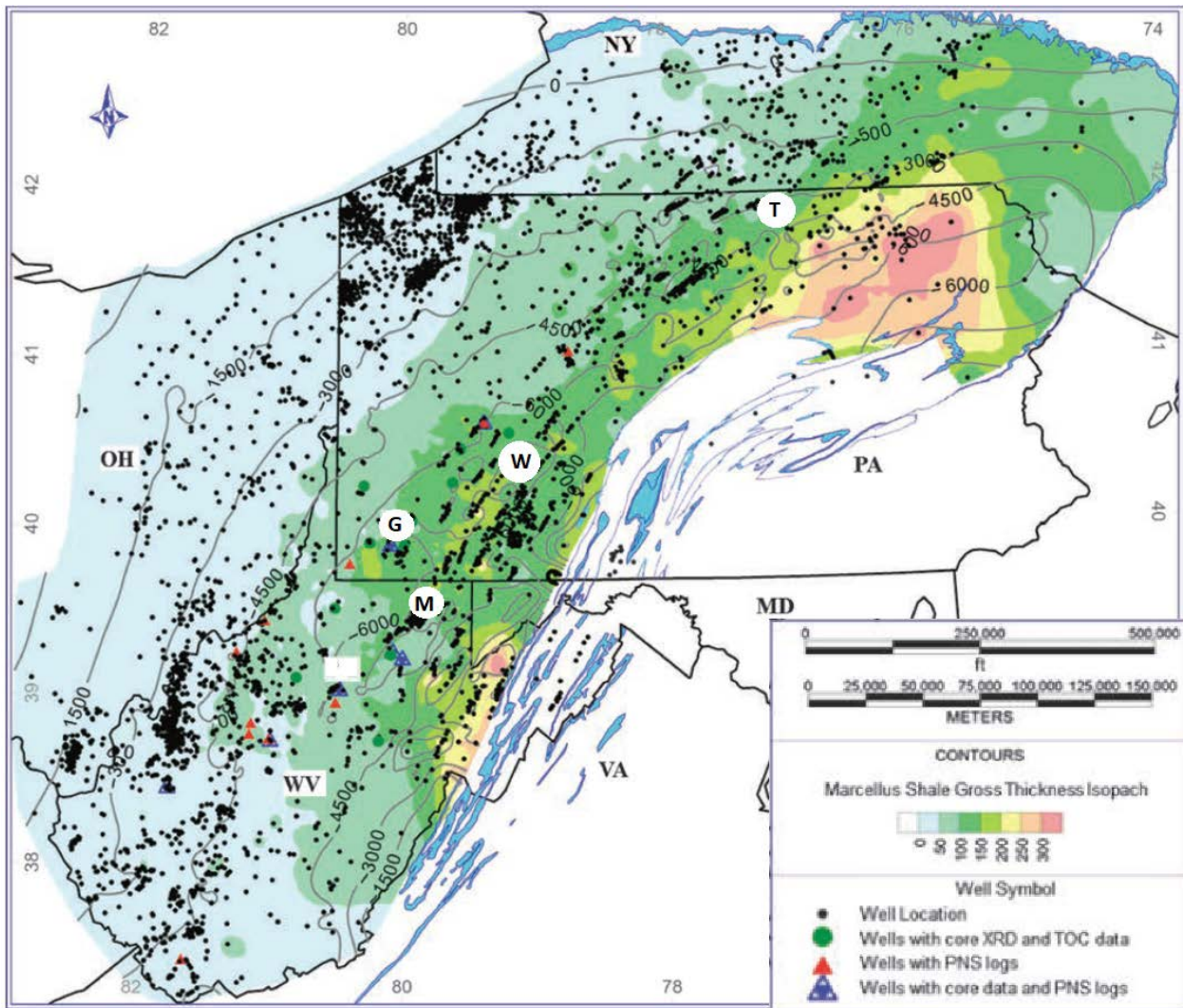


Figure 11: Depth and thickness map of the Marcellus Shale, with a 50 ft. isopach contour, a 1500 ft. depth contour, and sampling areas marked: M - MSEEL, G - Greene Co., W - Westmoreland Co., T - Tioga Co. (modified from Wang and Carr, 2013)

Marcellus Shale returned water is known to have very high Ba concentrations (Hayes, 2009; Chapman et al., 2012; Haluszczak et al., 2013; Engle and Rowan, 2014). As discussed in Chapter 1, this can have a detrimental effect on natural gas extraction, due to the potential fouling of the well from precipitation of barite (Paukert Vankeuren et al., 2017). A statistical analysis of Marcellus produced waters by Engle and Rowan (2014) showed that waters with the highest Ba content tended to also be sulfate-poor. Sequential extraction experiments on Marcellus Shale samples by Stewart et al. (2015) demonstrated that the majority of easily-extractable Ba in Marcellus Shale rock is held on cation exchange sites on the surfaces of minerals and organic matter, suggesting that this could be a source of Ba in Marcellus Shale returned water. Renock et al. (2016) suggested that high Ba levels in Marcellus Shale returned water result from reductive weathering while the injected fluid is in contact with the shale. However, Stewart et al. (2015) note that unrealistically high rock:water ratios may be required to explain the observed Ba levels in Marcellus shale produced water. In addition, Rowan et al. (2015) suggest that the late-stage produced waters represent pre-existing brines within or near the Marcellus Shale. Motivated in part by the importance of determining the source of Ba in produced water, I report barium isotope data from Marcellus Shale leachates (including both exchangeable cations and carbonate cement), produced water from Marcellus Shale wells, and additional produced water samples from conventional oil and gas wells in Pennsylvania.

### **3.2 GEOLOGY OF THE MARCELLUS SHALE**

The Marcellus Shale is a Middle Devonian organic-rich black shale underlying portions of New York, Pennsylvania, Ohio, West Virginia, and Virginia (Figure 11). It consists of two primary members, the upper Oatka Creek and lower Union Springs, separated by a small limestone

interval, the Purcell Limestone (Lash and Blood, 2014). The Union Springs member is the usual target of gas exploration. The Marcellus is part of the Hamilton Group, which also includes the overlying Mahantango Formation, a gray shale. It is underlain by the Onondaga Limestone (Figure 12). In the heavily-drilled southwestern Pennsylvania region, the shale is around 6000 ft below the surface and 100-200 ft thick (Wang and Carr, 2013).

The Marcellus Shale was deposited during the mid Devonian in a sheltered inland sea basin as part of the Catskill Delta about 30° south of the equator (Figure 13). Clastic sediments were derived from the Acadian highlands to the southeast (Lash and Blood, 2014).

### **3.3 SAMPLE MATERIALS**

#### **3.3.1 Core and produced water from the MSEEL Drilling Site**

A series of Marcellus flowback/produced water and core samples used in this study were obtained from a drilling site within the Marcellus Shale Energy and Environment Laboratory (MSEEL), a hydraulic fracturing field site run by a variety of institutions, including the National Energy Technology Laboratory (NETL), West Virginia University, and the Ohio State University (Carr et al., 2017). The site includes four producing horizontal wells: two relatively low-producing wells that were drilled in 2011 (wells 4H and 6H), and two wells that were completed in December 2015 (wells 3H and 5H). Well 3H also had a complete vertical core taken (Sharma et al., 2017). The samples for this study came from well 3H, in the MIP pad, which is located near Morgantown, WV and 580 m laterally from the Monongahela River (Figure 14; Ziemkeiwicz, 2017). The natural gas produced from the wells is used in nearby Morgantown, and researchers have access to logs and samples. In addition, there are sampling

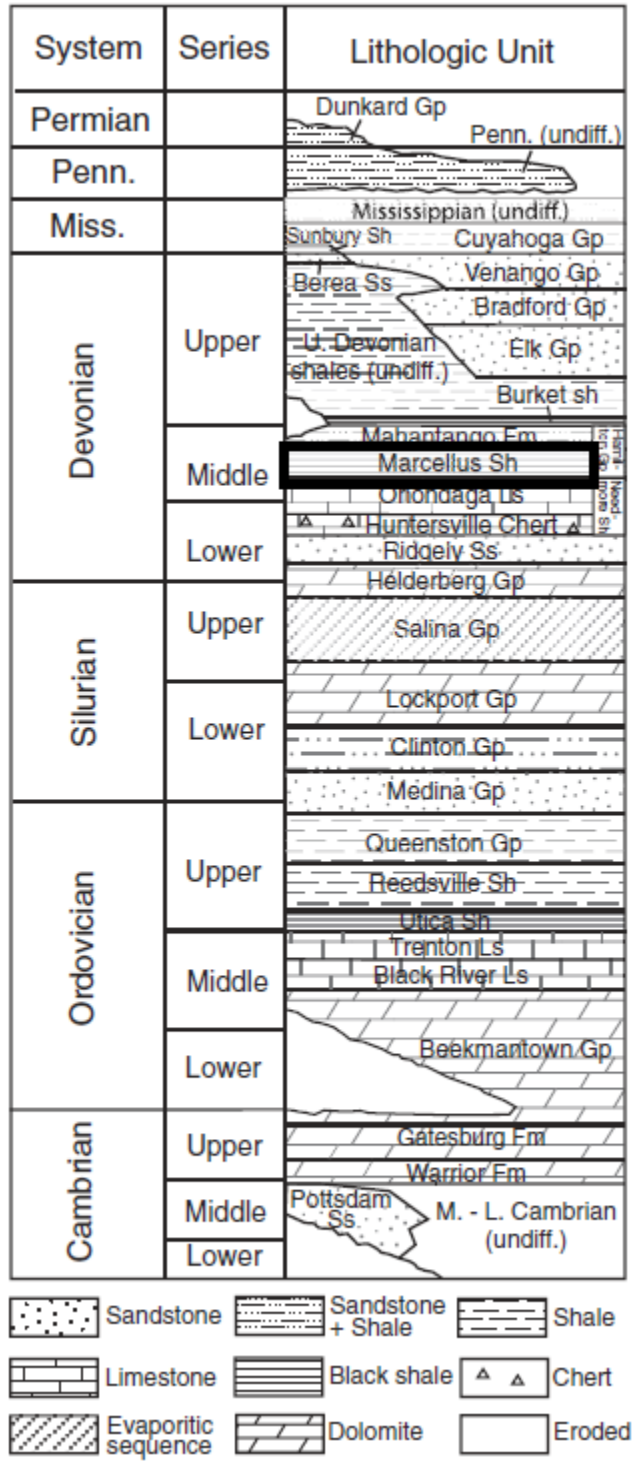


Figure 12: Cambrian through Permian stratigraphy in Pennsylvania (modified from Rowan et al., 2015)

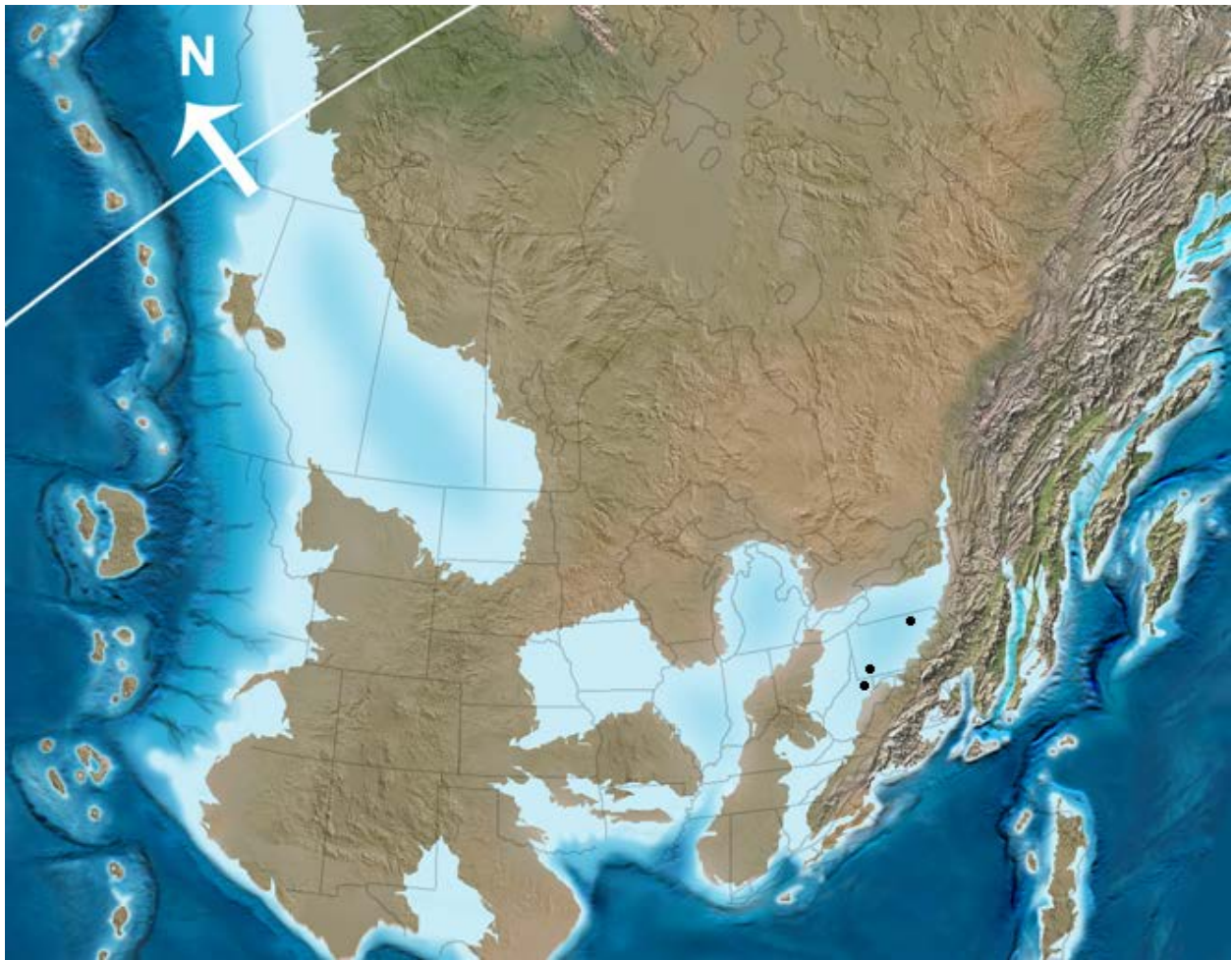


Figure 13: Paleogeographic reconstruction of North America, Middle Devonian; approximate paleolocation of study areas marked (modified from Blakey, 2017)

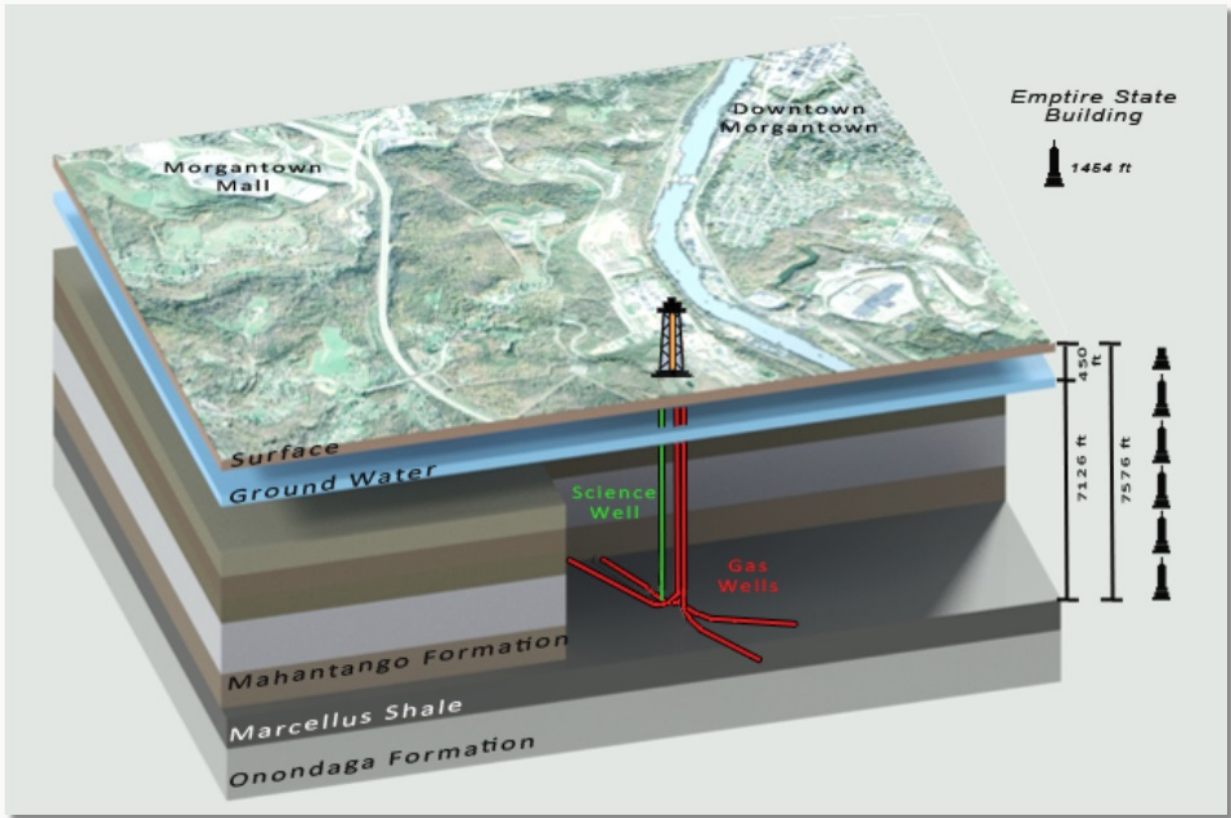


Figure 14: MSEEL well site and well schematic near Morgantown, WV (MSEEL, 2017)

stations upstream and downstream of the site on the river that have taken and continue to take water quality samples before, during, and after drilling and production (Ziemkiewicz, 2017).

Marcellus Shale rock samples were taken from core of well 3H at varying depths (7449.25, 7484.11, 7503.98, 7512.01, and 7534.04 feet below the surface) in an area where the Marcellus Shale extends from 7445 to 7557 feet. Rock samples were all powdered and then subjected to a sequential extraction procedure for exchangeable cations and carbonate before being processed through the columns as described below.

A time series of six water samples was taken from MSEEL's MIP 3H well starting just after flowback began. All water samples were filtered to 0.45  $\mu\text{m}$  and acidified with 2%  $\text{HNO}_3$ . Samples from December 10, 11, 13 of 2015 were taken prior to gas production. Samples from January 14, February 3 and April 12 of 2016 are waters co-produced with methane. The produced water samples were aliquoted before being processed through the columns in preparation for MC-ICP-MS analysis.

### **3.3.2 Produced water from other sites**

Eight additional produced water samples from around the state of Pennsylvania were analyzed. Produced water samples from three Middle Devonian Marcellus Shale gas wells were taken in Tioga County (SA14; see additional data in Rowan et al., 2015; Phan et al., 2016), Westmoreland County (WE-B18; Chapman et al., 2012; Phan et al., 2016), and Greene County (MO6 - vertical Marcellus, hydraulically fractured, ~7 years after initial fracturing; Kolesar Kohl et al., 2014; Phan et al., 2016). Three water samples were taken from wells producing from upper Devonian/ lower Mississippian strata: one from an unconventional well tapping the Burket Shale in Tioga County (ST46; Rowan et al., 2015; Phan et al., 2016) and two from conventional wells in Greene County (MO5 and MC1; Kolesar Kohl et al., 2014; Phan et al., 2016). Finally,

water samples from conventional wells tapping the Middle Silurian Newburg Sandstone (SILN-ND; Phan et al., 2016) and the Upper Silurian Lockport Dolomite (SILN-L; Phan et al., 2016) were each taken from northern Pennsylvania.

### **3.4 METHODS**

#### **3.4.1 Sequential extraction**

Rather than dissolving the entirety of the core samples, they were sequentially leached to extract barium from different reservoirs within the rock that are more likely to be accessible during hydraulic fracturing (Stewart et al., 2015; Phan, et al., 2015). In this study, we sought to extract Ba from the cation exchange sites on the surfaces of minerals and organic matter, which are thought to contain most of the accessible Ba (Stewart et al., 2015; Renock et al., 2016), and from the carbonate cement fraction.

For the cation exchange sites, ammonium acetate buffered to a pH of 8.0 was added to powdered rock in a 40:1 ratio (Stewart et al., 2001, 2015; Phan et al., 2015). The mixture was agitated for four hours and then centrifuged for ten minutes at 5000 rpm. The fluid was pipetted out and filtered at 0.45  $\mu\text{m}$ , and then the process was repeated with a 30 minute agitation time.

Acetic acid (1.0 M) was used to dissolve the carbonate fraction of the samples, while minimizing dissolution of silicate components (Stewart et al., 2001, 2015; Phan et al., 2015). It was added in a 40:1 ratio to the residuum of the previous step, agitated vigorously, and then allowed to digest for thirty minutes. The mixture was allowed to vent built-up carbon dioxide and then was constantly agitated for four hours, pausing to vent every thirty minutes. The fluid was pipetted out and filtered to 0.45  $\mu\text{m}$ .

All leachate samples were evaporated to dryness in a HEPA-filtered hood, redissolved in ultraclean 2% nitric acid, and analyzed for Ba concentration by ICP-MS.

### **3.4.2 Chemistry and mass spectrometry**

Aliquots of 1-5  $\mu\text{g}$  of Ba were taken from the leachate solutions and the produced waters. The appropriate amount of  $^{135}\text{Ba}$ - $^{137}\text{Ba}$  double spike was added as described in Chapter 2. The aliquots were evaporated to dryness and redissolved in 2.0 N HCl for cation column separation. After the column procedure, the Ba cut was evaporated to dryness and redissolved in ultrapure 2%  $\text{HNO}_3$  for MC-ICP-MS analysis.

All samples were analyzed on a Neptune Plus MC-ICP-MS. The MSEEL flowback/produced water samples (except 3H04) were analyzed using the standard sample introduction system, with  $^{136}\text{Xe}$  corrected by subtracting the full background at mass 136, but not monitored during the runs. All other samples were analyzed using the Apex® sample introduction system, with  $^{136}\text{Xe}$  monitored continuously during the run by measuring  $^{131}\text{Xe}$ . Repeated measurement of the NIST 3104a standard yielded no significant variation over the course of the analyses, so samples were normalized to the average value of the standard. Duplicate runs were carried out within each analytical session on the MC-ICP-MS, and all fell within error of the original analysis.

## **3.5 RESULTS**

### **3.5.1 Shale leachates**

The  $\delta^{138}\text{Ba}$  values of exchangeable Ba (ammonium acetate extracts; Table 2) from Marcellus Shale core material from different depths fall within a relatively narrow range of 0.48-0.58‰ (average of duplicates; Table 2) and essentially within analytical uncertainty of one another.

Table 2:  $\delta^{138}\text{Ba}$  of extracted samples

Sample	[Ba], $\mu\text{g per g}$ sample leached	$\delta^{138}\text{Ba}$	2 S.E.
<i>Cation Exchange Sites</i>			
E7449	289	0.451	$\pm 0.053$
duplicate		0.508	$\pm 0.063$
E7484	431	0.603	$\pm 0.047$
duplicate		0.566	$\pm 0.047$
E7503	273	0.532	$\pm 0.064$
duplicate		0.522	$\pm 0.061$
E7512	334	0.594	$\pm 0.052$
duplicate		0.486	$\pm 0.056$
E7534	371	0.527	$\pm 0.062$
duplicate		0.552	$\pm 0.048$
<i>Carbonate Fractions</i>			
C7449	2.48	0.473	$\pm 0.042$
duplicate		0.460	$\pm 0.042$
C7484	2.72	0.567	$\pm 0.050$
duplicate		0.579	$\pm 0.040$
C7503	5.12	0.546	$\pm 0.052$
duplicate		0.543	$\pm 0.041$
C7512	3.60	0.600	$\pm 0.046$
duplicate		0.577	$\pm 0.044$
C7534	6.13	0.596	$\pm 0.038$
duplicate		0.599	$\pm 0.042$

These values are generally higher than those of bulk silicate rocks that have been measured to date ( $\delta^{138}\text{Ba} = -0.07$  to  $0.19\text{‰}$ ; see Chapter 1) but are similar to modern seawater (Figure 15; von Allmen et al., 2010; Horner et al., 2015; Cao et al., 2016; Pretet et al., 2016; Bates et al., 2017).

The carbonate (acetic acid leachate)  $\delta^{138}\text{Ba}$  values also fall within a narrow range ( $0.47$ - $0.60\text{‰}$ ) that overlaps significantly with the exchangeable Ba (Table 2). Neither the exchangeable nor the carbonate  $\delta^{138}\text{Ba}$  exhibits a systematic shift with depth in the core (Figure 16).

As demonstrated previously for other Marcellus Shale samples (Stewart et al., 2015; Renock et al., 2016), most of the accessible Ba is in the exchangeable sites of the shale, with concentrations up to  $430 \mu\text{g Ba per g}$  of rock leached (Table 2). The carbonate contains less Ba by a factor of  $\sim 10^2$  ( $3.5 \mu\text{g}$  of barium in carbonate per g of leached rock versus  $325 \mu\text{g}$  on cation exchange). While the  $\delta^{138}\text{Ba}$  of the exchangeable fraction seems to exhibit a slight correlation with Ba concentration (Figure 17), the same is not seen in the carbonate.

### **3.5.2 Produced Waters**

Concentrations of Ba from the flowback/produced water time series from the MSEEL site show the expected trend of increasing Ba concentration over time (Table 3; Figure 18a) The  $\delta^{138}\text{Ba}$  values fall within a relatively narrow range of  $0.81$ - $0.99\text{‰}$ , and appear to show a decrease after day 1, followed by a gradual increase to day 56 and another decrease by day 489 (Figure 18b). All of the MSEEL produced water  $\delta^{138}\text{Ba}$  values are significantly higher (outside of analytical error) than the MSEEL exchangeable and carbonate values:  $\delta^{138}\text{Ba} = 0.808$ — $1.020\text{‰} \pm 0.055\text{‰}$  2 S.E for the produced waters and  $0.451$ — $0.603\text{‰} \pm 0.050\text{‰}$  in the extracted fractions.

Other produced water samples from Marcellus Shale wells have positive  $\delta^{138}\text{Ba}$  values, ranging from  $0.60\text{‰}$  in Greene County, PA, to  $1.52\text{‰}$  in Westmoreland County, PA. The latter

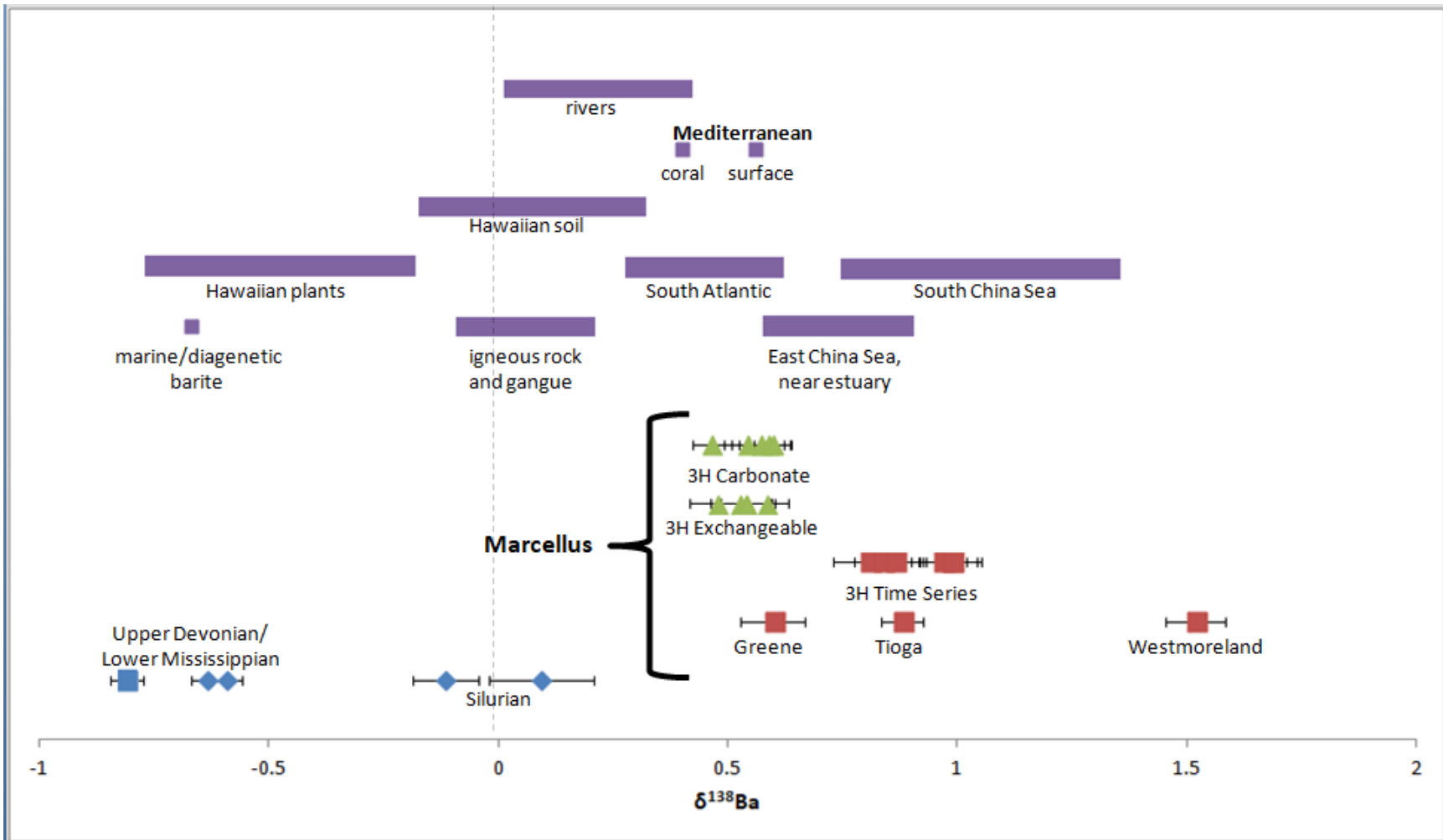


Figure 15: Summary of  $\delta^{138}\text{Ba}$  results with some comparative literature values. Conventional well samples are diamonds, unconventional are squares, leachates are triangles. Data not from this study are from von Allmen et al., 2010, Bullen and Chadwick, 2015, Cao et al., 2015, Horner et al., 2015, Nan et al., 2015, and Pretet et al., 2015)

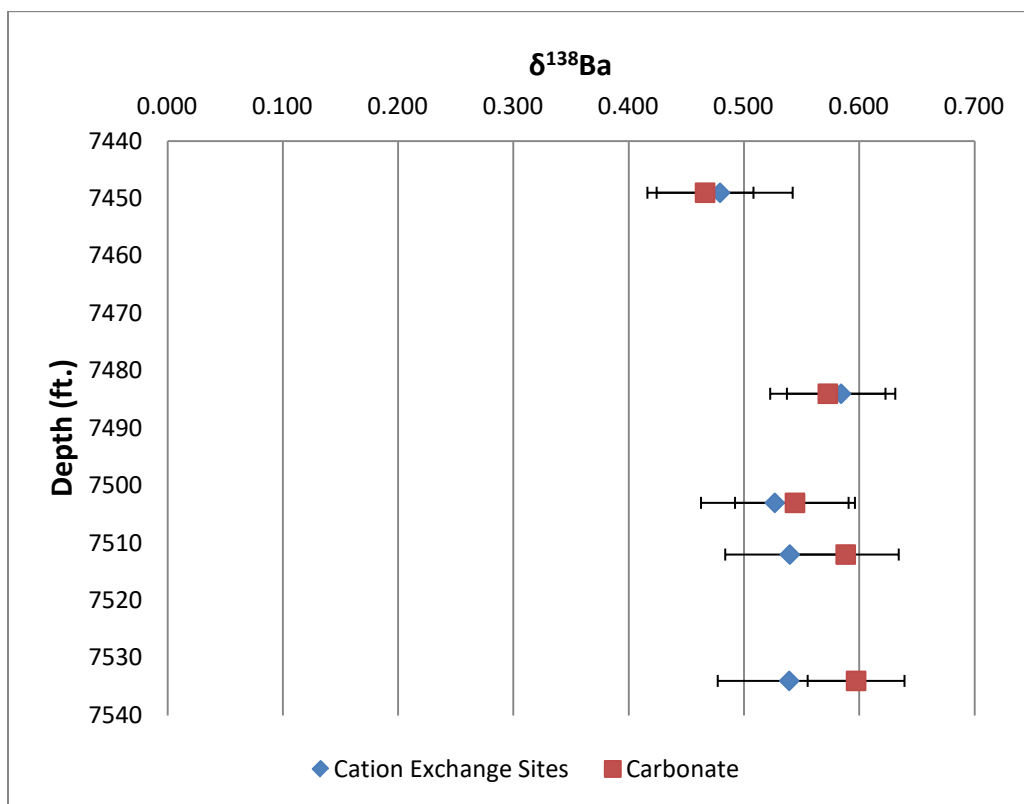


Figure 16:  $\delta^{138}\text{Ba}$  of leachates by depth

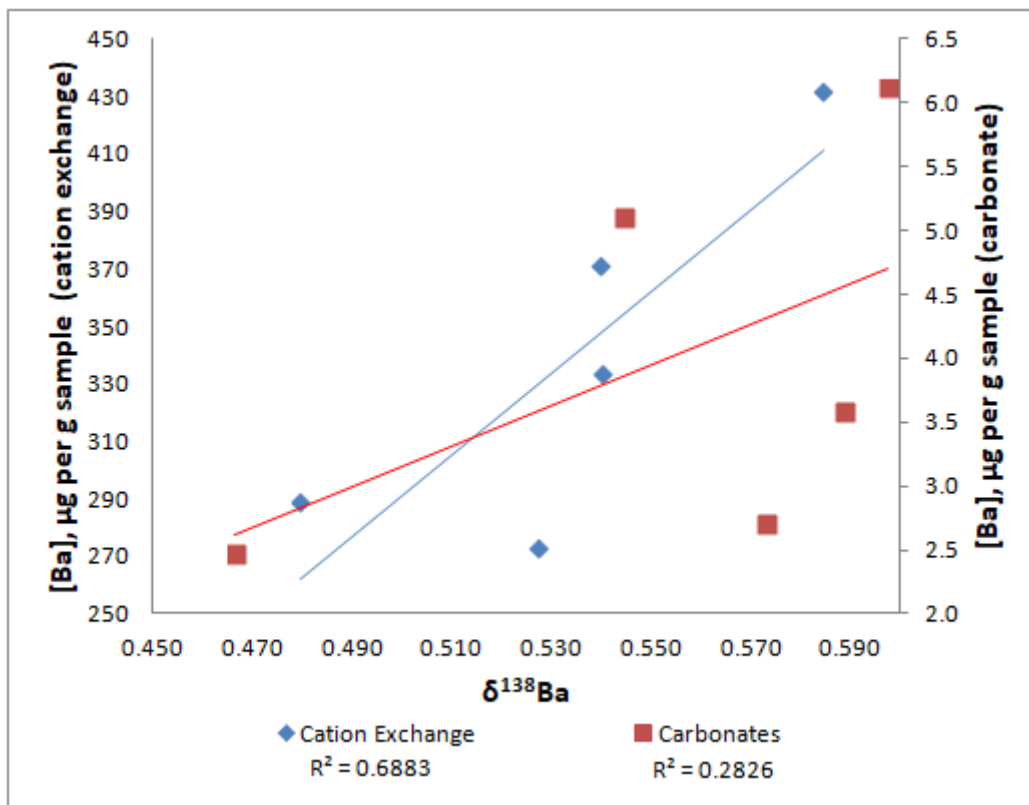


Figure 17: Correlation of exchangeable and carbonate  $\delta^{138}\text{Ba}$  with Ba concentration ( $\mu\text{g}$  of Ba per g of sample leached)

Table 3:  $\delta^{138}\text{Ba}$  of produced waters

Sample	Description	[Ba], mg/L	$\delta^{138}\text{Ba}$	2 S.E.
<i>Time Series</i>				
3H12102015	Day 1	240	1.02	$\pm 0.055$
duplicate			0.954	$\pm 0.045$
3H12112015	Day 2	267	0.808	$\pm 0.077$
3H12132015	Day 4	702	0.837	$\pm 0.063$
3H01142016	Day 36	2650	0.967	$\pm 0.052$
3H02032016	Day 56	3504	0.975	$\pm 0.061$
duplicate			1.00	$\pm 0.063$
3H04122017	Day 489	6656	0.889	$\pm 0.043$
duplicate			0.839	$\pm 0.053$
<i>Unconventional Wells</i>				
MO6	MD Vertical Marcellus, Greene	2311	0.658	$\pm 0.059$
duplicate			0.565	$\pm 0.063$
MO6	chemistry duplicant		0.603	$\pm 0.068$
duplicate			0.567	$\pm 0.070$
SA147	MD Marcellus, Tioga	16500	0.885	$\pm 0.046$
duplicate			0.873	$\pm 0.045$
S2H	MD Marcellus, Westmoreland	2700	1.57	$\pm 0.064$
duplicate			1.47	$\pm 0.051$
ST460	UD/LM Burket Shale, Tioga	5320	-0.816	$\pm 0.031$
duplicate			-0.806	$\pm 0.036$
<i>Conventional Wells</i>				
COG	M-SN Newburg Sandstone, Tioga	10.0	0.032	$\pm 0.104$
duplicate			0.154	$\pm 0.115$
LP 3515	U-SN Lockport Dolomite, Tioga	0.58	-0.123	$\pm 0.071$
duplicate			-0.107	$\pm 0.056$
MO5	UD/LM, Greene	235	-0.619	$\pm 0.032$
duplicate			-0.647	$\pm 0.036$
MC1	UD/LM, Greene	97.0	-0.608	$\pm 0.027$
duplicate			-0.574	$\pm 0.034$

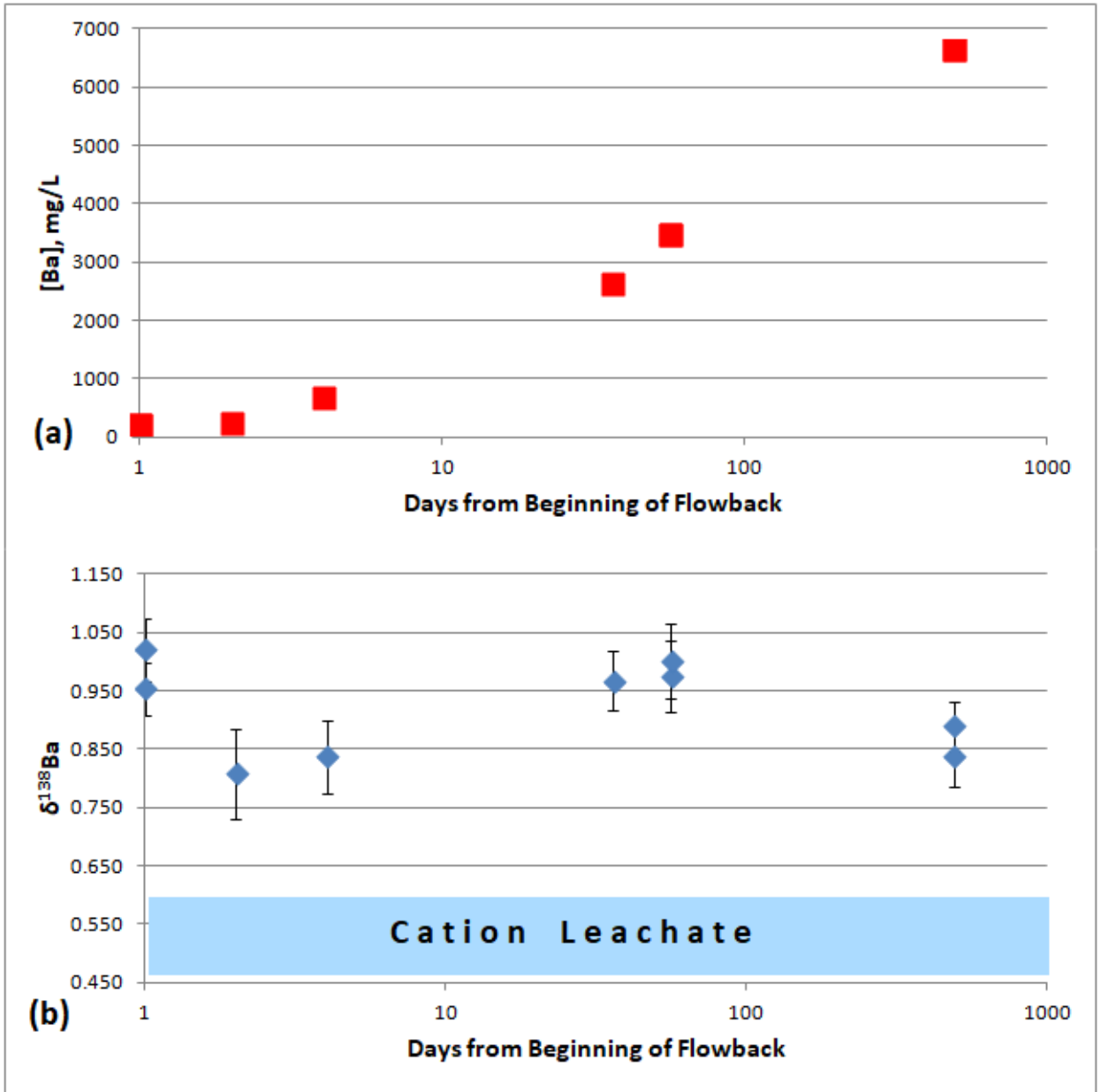


Figure 18: Plot of (a) [Ba] and (b)  $\delta^{138}\text{Ba}$  against day of sample collection after initiation of flowback for the MSEEL 3H well; range of  $\delta^{138}\text{Ba}$  values for the cation leachates shown in the shaded area

value appears unusually high, but Chapman et al. (2012) found that produced waters from the same wells (including the sample analyzed here) also yielded anomalously high  $^{87}\text{Sr}/^{86}\text{Sr}$  ratios.

Produced water from conventional wells drilled into Silurian sandstone and dolomite underlying the Marcellus Shale (COG and LP 3515; Table 3) yield  $\delta^{138}\text{Ba}$  values significantly lower than those of hydraulically fractured Marcellus Shale wells, ranging from -0.12‰ to 0.09‰. Produced water from Upper Devonian/Lower Mississippian units overlying the Marcellus Shale yield even lower  $\delta^{138}\text{Ba}$  values (-0.81‰ to -0.59‰). Of these, sample ST46 is extracted from an unconventional Burket Shale well, while the other two are from conventional sandstone reservoirs.

## 3.6 DISCUSSION

### 3.6.1 Source of Ba in shale produced water

The  $\delta^{138}\text{Ba}$  values of exchangeable sites and carbonate cement within the Marcellus Shale at the MSEEL site in West Virginia fall within the range measured in Ba dissolved in modern seawater, but are significantly below values measured in flowback and produced waters from the same well (Figure 15). This suggests that Ba in the produced water was not derived directly from interaction of injected fluids with exchangeable sites in the shale, but may come from a separate source. This source could be (1) micro-barite within the shale that is attacked by high ionic strength waters (Renock et al, 2106), (2) pre-existing formation water in lenses or fractures within the shale (e.g., Rowan et al., 2015), or (3) overlying or underlying units tapped by hydraulic fracturing (e.g., Stewart et al., 2015).

An alternative explanation is that Ba isotopes fractionate during interaction with the fracturing fluid. A typical ion exchange reaction would be expected to preferentially extract light (low-  $\delta^{138}\text{Ba}$ ) Ba, which should yield a produced water with lower  $\delta^{138}\text{Ba}$  than that on the exchangeable sites. For our samples at the MSEEL site, we see the opposite effect, where the flowback and produced water is heavier (even early in the flowback sequence) than the associated exchangeable Ba. Therefore, we suggest it is unlikely that the difference is caused by mass fractionation during water-rock exchange.

### **3.6.2 Source of Ba in shale exchangeable sites and carbonate**

The Marcellus Shale was deposited in a shallow epicontinental seaway, west of the incipient Acadian Mountains and north of a set of shallow sills that restricted full circulation with the open ocean during the Middle Devonian Period. The source of Ba reaching the sea floor is likely to be a combination of continentally-derived sediments and possibly barite produced in the water column due to biological activity. The  $\delta^{138}\text{Ba}$  values on the exchange sites and within carbonate cement are broadly similar to the range of values seen in modern seawater, although marine bio-barite is expected to be ~0.3‰ lighter than coexisting seawater (Figure 15; von Allmen et al., 2010). The Marcellus exchangeable and carbonate barium is isotopically similar to that seen at the bottom of the East China Sea near the Changjiang estuary where there are high riverine inputs and high surface  $\delta^{138}\text{Ba}$  values (Cao et al., 2016). This may be an analog for the Marcellus interior seaway with potentially high riverine inputs from the newly uplifting eastern Acadian Mountains. Given the general lack of Ba isotope data on potential sources (including Middle Devonian seawater), additional work will be required to determine the source of labile Ba in shale.

### 3.6.3 Ba isotope variations in produced water

Marcellus shale produced waters from as far north as Tioga County, Pennsylvania, and as far south as Morgantown, West Virginia, appear to have higher  $\delta^{138}\text{Ba}$  values (0.6 to 1.5‰) than those of other produced waters in the Appalachian Basin, including from below the Marcellus (-0.1 to 0.1‰) and above (-0.8 to -0.6‰). The low  $\delta^{138}\text{Ba}$  values of Upper Devonian/Lower Mississippian produced waters are particularly intriguing, as the only natural samples reported to date with values this low are vegetation samples from Hawaii (Bullen and Chadwick, 2015), and one sample of marine barite from the Demerara Rise interpreted to be diagenetic (von Allmen et al., 2010). These data suggest distinct origins for Marcellus and other formation waters, but to pinpoint these sources requires more data to determine the full range of  $\delta^{138}\text{Ba}$  values in natural environments.

While we cannot yet determine the precise source of Ba in produced waters, the difference in  $\delta^{138}\text{Ba}$  between produced waters from the Marcellus Shale and those from overlying formations suggests the possibility that Ba isotopes could be used to “fingerprint” wastewater from different types of oil and gas wells and to identify the source of migrating subsurface brine. Strontium, lithium and boron isotopes have been previously shown to vary systematically between Marcellus Shale waters and those of overlying units (Chapman et al., 2012; Warner et al., 2012, 2014; Macpherson et al., 2014; Phan et al., 2016), but the difference appears to diminish somewhat in the northern part of the Appalachian Basin. If the Ba isotope differences are related to distinct evolutionary pathways of different formation waters, the differences could remain robust regardless of geographic location.

## 4.0 CONCLUSIONS

Barium in the Marcellus Shale has a general range of  $\delta^{138}\text{Ba}$  0.598-0.988‰ but is anomalously high in Westmoreland County, an area that also exhibits anomalous strontium isotope composition. Sequentially extracted cation exchange and carbonate samples from a drilled core had values 0.22-0.52‰ lighter than produced water from the same well, suggesting that injected water-rock interactions are not the primary source of barium in Marcellus produced waters. A time series of produced water taken from the well between the first day of flowback to well over a year later showed no trend in  $\delta^{138}\text{Ba}$  values, meaning Ba in flowback had a consistent primary source. There is much more barium in exchangeable cation sites (2.48-6.13  $\mu\text{g}$  per gram of leached sample) than in carbonate cement (272.91-431.46  $\mu\text{g}$  per gram of leached sample).

The  $\delta^{138}\text{Ba}$  of adjacent units are distinct from the Marcellus. Produced water from older Silurian units range from -0.633‰ to 0.093‰, and those from younger Upper Devonian/Lower Mississippian units go from -0.811‰ to -0.591‰ for both conventional and unconventional wells.

Continuation of this work could include further study of possible Ba sources to produced water. Drilling mud (which often contains barite as a major component) is a potential source of contamination, and ongoing work is measuring the isotopic composition of Ba found there. The injection fluid should be analyzed, but it is not expected to contribute much barium after the first day or two of flowback due to its much lower Ba concentration. It is possible evaporates from

the Silurian Salina Group could contribute TDS produced waters beneath the Marcellus, although this is not likely to be a major source of barium. The barium contained within shale silicate minerals is not expected to be easily available during water-rock interaction (Renock et al., 2016), but whole-rock shale data could provide valuable information on deposition, and some silicate contribution to the produced water Ba budget cannot be ruled out. Additional leaching with high-temperature, high-ionic strength fluids also releases further barium (Renock et al., 2016), so this should also be considered. Finally, barium isotope measurements of different types of produced waters and reservoir rocks within and outside of the Appalachian Basin would provide a valuable baseline for future Ba isotope studies of hydrocarbon-bearing sedimentary systems.

## APPENDIX

### STANDARD OPERATING PROCEDURE OF LOADING AND ELUTION OF BARIUM CATION COLUMNS

Purpose of Procedure: To collect purified separated of Ba from a dissolved sample solution

#### Materials

- Acid cleaned 15 mL centrifuge tubes (one per sample)
- For produced water samples, acid cleaned 15 mL Teflon containers (one per sample)
- For extracted samples, acid cleaned 30 mL Teflon containers (one per sample)
- For extracted samples, acid cleaned 30 mL Teflon containers (one per sample)

#### Reagents

- Cleaned AG-50W, 200-400 mesh 8% cross-linkage cation exchange resin
- Milli-Q water
- 2.0 N HCl (ultrapure)
- 4.0 N HCl (ultrapure)
- Concentrated HCl (ultrapure)
- 2% HNO<sub>3</sub> (ultrapure)
- Concentrated HNO<sub>3</sub> (ultrapure)

#### I. Preparation

1. Gather centrifuge tubes and the appropriate number of Teflon vials depending on sample type.
2. Ensure all vials and tubes are acid cleaned and labeled appropriately. Weigh each (only one decimal place for the centrifuge tubes; four otherwise).
3. Check normality of the 2.0 and 4.0 N HCl. Adjust as needed.

## II. Column Chemistry – Main Clean Lab

For all samples:

1. Begin with sample (already spiked if required) evaporated to dryness in Teflon.
2. Add 1 mL of concentrated HCl. Use only ultrapure acid throughout chemistry.
3. Sonicate the sample for at least 10 minutes to assist dissolution of the sample into acid.
4. Dry the sample again.
5. Add 0.5 mL of 2.0 N HCl.
6. Sonicate the sample for another 10 minutes.
7. Begin microcolumn preparation:
  - a. Gather the required number of clean microcolumns and place them in the stand with a waste beaker below each. Make sure the top of the frit is 6 cm below the bottom of the column reservoir.
  - b. For each microcolumn, fill partially with Milli-Q water and begin flow.
  - c. Add resin to the water and allow it to fill the column until the top of the resin is just into the bottom of the reservoir.
  - d. Make sure there are no bubbles in the resin—stir it up with a little more water if needed. Pipette out excess water, but do not at any time allow the resin to dry.

- e. Carefully add 0.5 mL of 4.0 N HCl to the edges of the reservoir, and allow it to run through.
  - f. Repeat this with 2 mL of 4.0 N HCl, then an additional 4 mL.
  - g. Do this again with 0.5 mL, 2 mL, and then 4 mL of 2.0 N HCl.
8. Add the sample carefully to the edges of the reservoir and allow it to run through.
  9. Add 1 mL 2.0 N HCl to the column.
  10. Diverge here, depending on sample type.

Produced Water Samples:

1. Add an additional 14 mL 2.0 N HCl and allow it to filter through. Be sure not to let the resin dry out.
2. Remove the waste beakers and dispose of the acid properly. Put an acid cleaned and labeled Teflon container under each column.
3. Add 10 mL of 2.0 N HCl. Collect this as the sample cut.
4. Dry the sample.
5. Add 1 mL of concentrated HNO<sub>3</sub>.
6. Sonicate for 10 minutes, and then dry the sample again.
7. Add 2 mL 2% HNO<sub>3</sub> per expected µg of barium.
8. Sonicate the sample for 10 minutes, and then move it to an acid cleaned and labeled 15 mL centrifuge tube. Add more 2% HNO<sub>3</sub> if needed.

*Sequentially Extracted Samples:*

1. Add an additional 15 mL 2.0 N HCl and allow it to filter through. Be sure not to let the resin dry out.

2. Remove the waste beakers and dispose of the acid properly. Put an appropriately-sized acid cleaned and labeled Teflon container under each column.
3. Add 22 mL of 2.0 N HCl. Collect this as the sample cut.
4. Dry the sample.
5. Add 0.5 mL of 2.0 N HCl, and then sonicate for 10 minutes.
6. Empty the used resin from columns and dispose of it, then add new resin and condition it as described above.
7. Add 1 mL of 2.0 N HCl and allow it to run through (as in step 9 above).
8. Add 15 mL of 2.0 N HCl and allow it to run through.
9. Remove the waste beakers and dispose of the acid properly. Put an appropriately-sized acid cleaned and labeled Teflon container under each column.
10. Add 14 mL of 2.0 N HCl. Collect this as the sample cut.
11. Dry the sample.
12. Add 1 mL of concentrated HNO<sub>3</sub>.
13. Sonicate for 10 minutes, and then dry the sample again.
14. Add 2 mL 2% HNO<sub>3</sub> per expected μg of barium.
15. Sonicate the sample for 10 minutes, and then move it to an acid cleaned and labeled 15 mL centrifuge tube. Add more 2% HNO<sub>3</sub> if needed.

## BIBLIOGRAPHY

- von Allmen, K., Böttcher, M.E., and Samankassou, E. 2010. Barium isotope fractionation in the global barium cycle: First evidence from barium minerals and precipitation experiments. *Chemical Geology*, 277: 70-77.
- Balashov, V.N., Engelder, T., Gu, X., Fantle, M.S., and Brantley, S.L. 2014. A model describing flowback chemistry changes with time after Marcellus Shale hydraulic fracturing. *AAPG Bulletin*, 99(1): 143-154.
- Barbot, E., Vidic, N.S., Gregory, K.B., and Vidic, R.D. 2013. Spatial and Temporal Correlation of Water Quality Parameters of Produced Waters from Devonian-Age Shale following Hydraulic Fracturing. *Environmental Science and Technology*, 47: 2562-2569.
- Bates, S.L., Hendry, K.R., Pryer, H.V., Kinsley, C.W., Pyle, K.M., Woodward, M.S., and Horner, T.J. 2017. Barium isotopes reveal role of ocean circulation on barium cycling in the Atlantic. *Geochimica et Cosmochimica Acta*, 204: 286-299.
- Blakey, R., 2017. Middle Devonian. Paleogeography and Geologic Evolution of North America: Images that track the ancient landscapes of North America. Accessed 14 Nov, 2017. Available at: <http://www2.nau.edu/rcb7/nam.html>.
- Böttcher, M.E., Geprägs, P., Neubert, N., von Allmen, K., Pretet, C., Samankassou, E., and Nägler, T.F. 2012. Barium isotope fractionation during experimental formation of the double carbonate  $\text{BaMn}[\text{CO}_3]_2$  at ambient temperature. *Isotopes in Environmental and Health Studies*, doi: 10.1080/10256016.2012.673489.
- Bullen, T. and Chadwick, O. 2015. Ca, Sr and Ba stable isotopes reveal the fate of soil nutrients along a tropical climosequence in Hawaii. *Chemical Geology*, 422: 25-45.
- Cao, Z., Siebert, C., Hathorne, E.C., Dai, M., and Frank, M. 2016. Constraining the oceanic barium cycle with stable barium isotopes. *Earth and Planetary Science Letters*, 434: 1-9.
- Capo, R.C., Stewart, B.W., Rowan, E.L., Kolesar Kohl, C.A., Wall, A.J., Chapman, E.C., Hammack, R.W., Schroeder, K.T., 2014. The strontium isotopic evolution of Marcellus Formation produced waters, southwestern Pennsylvania. *International Journal of Coal Geology*, 126: 57-63.
- Carr, T.R., Wilson, T.H., Kavousi, P., Amini, S., Sharma, S., Hewitt, J., Costello, I., Carney, B.J., Jordon, E., Yates, M., MacPhail, K., Uschner, N., Thomas, M., Akin, S., Magbagbeola, O., Morales, A., Johansen, A., Hogarth, L., Anifowoshe, O., Naseem, K., Hammack, R., Kumar, A., Zorn, E., Vagnetti, R., Crandall, D., NETL, USDoE. 2017. Insights from the Marcellus Shale Energy and Environment Laboratory (MSEEL). Unconventional Resources Technology Conference. Austin, TX, USA. 24-26 July, 2017. URTeC: 2670437.
- Chapman, E.C., Capo, R.C., Stewart, B.W., Kirby, C.S., and Hammack, R.W. 2012. Geochemical and Strontium Isotope Characterization of Produced Waters from Marcellus Shale Natural Gas Extraction. *Environmental Science and Technology*, 46(6): 3545-3553.
- Collins, A.G., 1975. *Geochemistry of Oilfield Waters*: New York, Elsevier, p. 496.

- Dodson, M.H. 1963. A theoretical study of the use of internal standards for precise isotopic analysis by the surface ionization technique: Part I – General first-order algebraic solutions. *Journal of Scientific Instruments*, 40(6): 289.
- Dresel, P.E. and Rose, A.W. 2010. Chemistry and Origin of Oil and Gas Well Brines in Western Pennsylvania. Pennsylvania Geological Survey, 4th ser., Open-File Report OFOG 10-01.0, p. 48.
- Engle, M.A. and Rowan, E.L. 2014. Geochemical evolution of produced waters from hydraulic fracturing of the Marcellus Shale, northern Appalachian Basin: A multivariate compositional data analysis approach. *International Journal of Coal Geology*, 126: 45-56.
- Eugster, O., Tera, F., and Wasserburg, G.J. 1969. Isotopic analyses of barium in meteorites and in terrestrial samples. *J. Geophys. Res.*, 74: 3897-3908.
- Finkel, M.L. and Law, A. 2011. The Rush to Drill for Natural Gas: A Public Health Cautionary Tale. *American Journal of Public Health*, 101(5): 784-785.
- Gonneea, M.E. and Paytan, A.I. 2006. Phase associations of barium in marine sediments. *Marine Chemistry*, 100: 124-135.
- Griffith, E.M. and Paytan, A. 2012. Barite in the ocean-occurrence, geochemistry and palaeoceanographic applications. *Sedimentology*, 59: 1817-1835.
- Ground Water Protection Council and ALL Consulting, 2009. Modern Shale Gas Development in the United States: A Primer, Oklahoma City, OK, [http://www.netl.doe.gov/technologies/oil-gas/publications/epreports/shale\\_gas\\_primer\\_2009.pdf](http://www.netl.doe.gov/technologies/oil-gas/publications/epreports/shale_gas_primer_2009.pdf).
- Haluszczak, L.O., Rose, A.W., and Kump, L.R. 2012. Geochemical evaluation of flowback brine from Marcellus gas wells in Pennsylvania, USA. *Applied Geochemistry*, 28: 55-61.
- Hanor, J.S. and McIntosh, J.C. 2006. Are secular variations in seawater chemistry reflected in the compositions of basinal brines? *Journal of Geochemical Exploration*, 86: 153-156.
- Hayes, T., 2009. Sampling and Analysis of Water Streams Associated with the Development of Marcellus Shale Gas. Report by the Gas Technology Institute, Des Plaines, IL. Marcellus Shale Coalition.
- Horner, T.J., Kinsley, C.W., and Nielsen, S.G. 2015. Barium-isotopic fractionation in seawater mediated by barite cycling and oceanic circulation. *Earth and Planetary Science Letters*, 430: 511-522.
- Jamieson, J.W., Hannington, M.D., Tivey, M.K., Hansteen, T., Williamson, N.M.B., Stewart, M., Fietzke, J., Butterfield, D., Frische, M., Allen, L., Cousens, B., and Langer, J. 2016. Precipitation and growth of barite within hydrothermal vent deposits from the Endeavour Segment, Juan de Fuca Ridge. *Geochimica et Cosmochimica Acta*, 173: 64-85.
- Kargbo, D.M., Wilhelm, R.G., and Campbell, D.J. 2010. Natural Gas Plays in the Marcellus Shale: Challenges and Potential Opportunities. *Environmental Science and Technology*, 44(15): 5679-5684.
- Kolesar Kohl, C.A., Capo, R.C., Stewart, B.W., Wall, A.J., Schroeder, K.T., Hammack, R.W., Guthrie, G.D., 2014. Strontium isotopes test long-term zonal isolation of injected and Marcellus Formation water after hydraulic fracturing. *Environmental Science and Technology*, 48: 9867-9873.
- Land, L.S. 1995. Na-Ca-Cl saline formation waters, Frio Formation (Oligocene), south Texas, USA: Products of diagenesis. *Geochimica et Cosmochimica Acta*, 59(11): 2163-2174.
- Land, L.S. and Macpherson, G.L. 1992. Origin of Saline Formation Waters, Cenozoic Section, Gulf of Mexico Sedimentary Basin. *AAPG Bulletin*, 76(9): 1344-1362.

- Lash, G.G. and Blood, D.R. 2014. Organic matter accumulation, redox, and diagenetic history of the Marcellus Formation, southwestern Pennsylvania, Appalachian basin. *Marine and Petroleum Geology*, 57: 244-263.
- Lü, Z., Liu, C., Liu, J., and Zhao, Z. 2003. Carbon, oxygen and boron isotopic studies of Huangbaishuwan witherite deposit at Ziyang and Wenyuhe witherite deposit at Zhushan. *Science in China (Series D)*, 46(12): 1273-1291.
- Macpherson, G.L. 1992. Regional Variations in Formation Water Chemistry: Major and Minor Elements, Frio Formation Fluids, Texas. *AAPG Bulletin*, 76(5): 740-757.
- Marcellus Shale Coalition (MSC). 2013. The Marcellus Shale: A Local Workforce with a National Impact. Fact Sheet. Available at: <http://www.MarcellusCoalition.org>
- Marcellus Shale Energy and Environment Laboratory (MSEEL). Outreach. Accessed Oct 24, 2017. Available at: <http://www.mseel.org>.
- Mavromatis, V., van Zuilen, K., Purgstaller, B., Baldermann, A., Nägler, T.F., and Dietzel, M. 2016. Barium isotope fractionation during witherite ( $\text{BaCO}_3$ ) dissolution, precipitation and at equilibrium. *Geochimica et Cosmochimica Acta*, 190: 72-84.
- McCulloch, M.T. and Wasserburg, G.J. 1978. Barium and neodymium isotopic anomalies in Allende meteorite. *Astrophysical Journal*, 220: L15-L19.
- McIntosh, J.C. Walter, L.M., and Martini, A.M. 2004. Extensive microbial modification of formation water geochemistry: Case study from a Midcontinent sedimentary basin, United States. *GSA Bulletin*, 116(5/6): 743-759.
- Miyazaki, T., Kimura, J., and Chang, Q. 2014. Analysis of stable isotope ratios of Ba by double-spike standard-sample bracketing using multiple-collector inductively coupled plasma mass spectrometry. *J. Anal. At. Spectrom.*, 29: 483-490.
- Ministry of Natural Gas Development (MNGD) and Minister Responsible for Housing (MRH), 2017. Conventional versus Unconventional Oil and Gas. Province of British Columbia. Accessed Nov 11, 2017. Available at: <https://www2.gov.bc.ca/gov/content/industry/natural-gas-oil/petroleum-geoscience>.
- Nan, X., Wu, F., Zhang, Z., Hou, Z., Huang, F., Yu, H., 2015. High-precision barium isotope measurements by MC-ICP-MS. *J. Anal. At. Spectrom.*, 30: 2307-2315.
- Nier, A.O. 1938. The isotopic constitution of strontium, barium, bismuth, thallium, and mercury. *Physical Review*, 54: 275.
- Oliver, J. 1986. Fluids expelled tectonically from orogenic belts: Their role in hydrocarbon migration and other geologic phenomena. *Geology*, 14: 99-102.
- Paukert Vankeuren, A.N., Hakala, J.A., Jarvis, K., Moore, J.E., 2017. Mineral reactions in shale gas reservoirs: Barite scale formation from reusing produced water as hydraulic fracturing fluid. *Environmental Science and Technology*, 51: 9391-9402.
- Phan, T.T., Capo, R.C., Stewart, B.W., Graney, J.R., Johnson, J.D., Sharma, S., and Toro, J. 2015. Trace metal distribution and mobility in drill cuttings and produced waters from Marcellus Shale gas extraction: Uranium, arsenic, barium. *Applied Geochemistry*, 50: 89-103.
- Poth, C.W., 1962. The occurrence of brine in western Pennsylvania. *Pennsylvania Geological Survey, Fourth Series, Bulletin M 47*, p 53.
- Pretet, C., van Zuilen, K., Nägler, T.F., Reynaud, S., Böttcher, M.E., and Samankassou, E. 2016. Constraints on barium isotope fractionation during aragonite precipitation by corals. *The Depositional Record*, 1(2): 118-129.

- Renock, D., Landis, J.D., and Sharma, M. 2016. Reductive weathering of black shale and release of barium during hydraulic fracturing. *Applied Geochemistry*, 65: 73-86.
- Rowan, E.L., Engle, M.A., Kraemer, T.F., Schroeder, K.T., Hammack, R.W. and Doughten, M.W. 2015. Geochemical and isotopic evolution of water produced from Middle Devonian Marcellus shale gas wells, Appalachian basin, Pennsylvania. *AAPG Bulletin*, 99(2): 181-206.
- Rudge, J.F., Reynolds, B.C., and Bourdon, B. 2009. The double spike toolbox. *Chemical Geology*, 265: 420-431.
- Russell, W.A., Papanastassiou, D.A., Tombrello, T.A., 1978. Ca isotope fractionation on the Earth and other solar system materials. *Geochimica Cosmochimica Acta*, 42: 1075-1090.
- Salminen, R. (ed.) 2005. *Geochemical Atlas of Europe. Part 1: Background Information, Methodology and Maps*. Espoo, Finland. Geological Survey of Finland. p. 71-77.
- Sharma, S., Carr, T.R., Mouser, P.J., Wrighton, K. Cole, D., Wilkins, M., Darrah, T., and Hakala, A. 2017. Biogeochemical Characterization of Core, Fluids, and Gas at MSEEL Site. Unconventional Resources Technology Conference. Austin, TX, USA. 24-26 July, 2017. URTeC: 2669965.
- Shen, D., Fu, G., Al-Saiari, H., Kan, A.T., and Tomson, M.B. 2009. Barite Dissolution/Precipitation Kinetics in Porous Media and in the Presence and Absence of a Common Scale Inhibitor. *SPE Journal*, September 2009: 462-471.
- Soeder, D.J. Sharma, S., Pekney, N., Hopkinson, L., Dilmore, R., Kutchko, B., Stewart, B., Carter, K., Hakala, A., and Capo, R. 2014. An approach for assessing engineering risk from shale gas wells in the United States. *International Journal of Coal Geology*, 126: 4-19.
- Stewart, B.W., Chapman, E.C., Capo, R.C., Johnson, J.D., Graney, J.R., Kirby, C.S., and Schroeder, K.T. 2015. Origin of brines, salts and carbonate from shales of the Marcellus Formation: Evidence from geochemical and Sr isotope study of sequentially extracted fluids. *Applied Geochemistry*, 60: 78-88.
- Terry, R.E. 2001. Enhanced Oil Recovery. *Encyclopedia of Physical Science and Technology*, 3rd ed. vol 18. Robert A. Meyers Ed., Academic Press. p. 503-518.
- Umemoto, S., 1962. Isotopic composition of barium and cerium in stone meteorites. *J. Geophys. Res.*, 67: 375-379.
- Wang, G. and Carr, T.R. 2013. Organic-rich Marcellus Shale lithofacies modeling and distribution pattern analysis in the Appalachian Basin. *AAPG Bulletin*, 97(12): 2173-2205.
- Warner, N.R., Jackson, R.B., Darrah, T.H., Osborn, S.G., Down, A., Zhao, K., White, A., Vengosh, A., 2012. Geochemical evidence for possible natural migration of Marcellus Formation brine to shallow aquifers in Pennsylvania. *Proc. Nat. Acad. Sci.*, 109: 11961-11966.
- Warner, N.R., Darrah, T.H., Jackson, R.B., Millot, R., Kloppmann, W., Vengosh, A., 2014. New tracers identify hydraulic fracturing fluids and accidental releases from oil and gas operations. *Environmental Science and Technology*, 48: 12552-12560.
- Wasserburg, G.J., Jacobsen, S.B., DePaolo, D.J., McCulloch, M.T., Wen, T., 1981. Precise determination of Sm/Nd ratios, Sm and Nd isotopic abundances in standard solutions. *Geochim. Cosmochim. Acta* 45: 2311-2323.
- Zagorski, W.A., Wrightstone, G.R., Bowman, D.C., 2012. The Appalachian Basin Marcellus gas play: Its history of development, geologic controls on production, and future potential as a world-class reservoir. In: Breyer, J.A. (Ed.), *Shale Reservoirs - Giant Resources for the 21st Century*, AAPG Memoir, 97: 172-200.

- Ziemkiewicz, P.F. 2017. The Marcellus Shale Energy and Environmental Laboratory (MSEEL): Water and Solid Waste Findings—Year One. Unconventional Resources Technology Conference. Austin, TX, USA. 24-26 July, 2017. URTeC: 2669914.
- van Zuilen, K., Müller, T., Nägler, T.F., Dietzel, M., and Kuesters, T. 2016. Experimental determination of barium isotope fractionation during diffusion and adsorption processes at low temperatures. *Geochimica et Cosmochimica Acta*, 186: 226-241.